

XVth Quark Confinement and the Hadron
Spectrum Conference
Cairns Convention Centre, Cairns, Queensland, Australia
19-24 August 2024 (inclusive)

How many vector charmonium(-like)
states from 4.2 to 4.35 GeV?



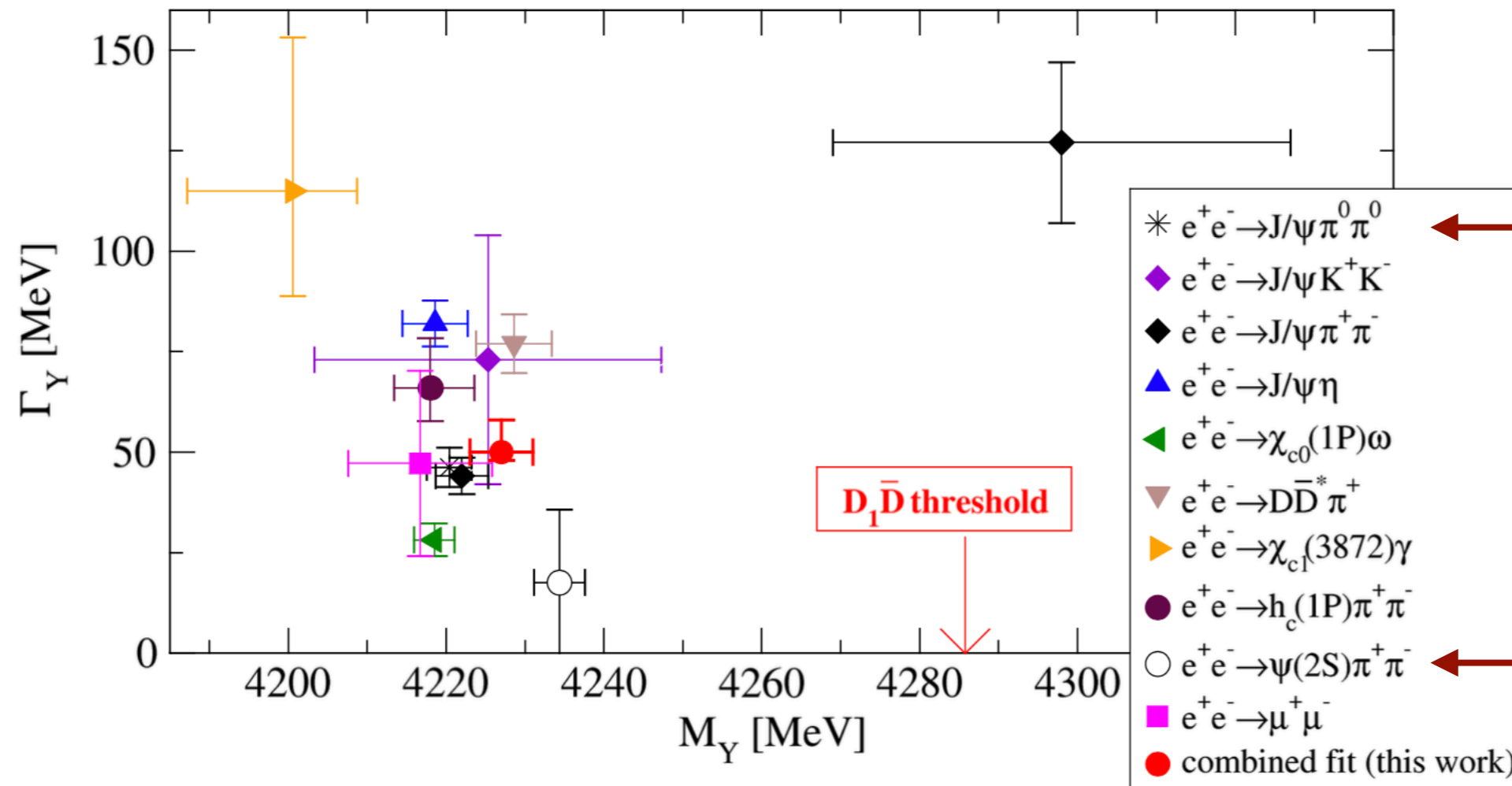
Qian Wang (王倩)
qianwang@m.scnu.edu.cn
19th-24th Aug. 2024



Vector charmonium(-like) states

Numerous states between 4.2 GeV and 4.35 GeV

Detten et al., PRD109(2024)116002



- BW resonance parameters in ten channels are not consistent
- An S-wave threshold $D_1 \bar{D}$ locates within this energy region
- Large statistic data from BESIII → a global fitting?

The status of vector charmonium(-like) states

The status of vector charmonium-like states

- Hybrid

Spectrum

Close et al., PLB628(2005)215, Kou et al., PLB628(2005)164,

Kalashnikova et al., PRD77(2008)054025, Berwein, et al., PRD92(2015)114019

Decay to spin singlet and disfavor hybrid

Brambilla et al., PRD107(2023)054034

- Hadrocharmonium

Talk by Abhishek Mohapatra on 19th (Mon)

Proposed to explain the $J/\psi\pi\pi$ lineshape

Dubynskiy et al., PLB666(2008)344

The mixing between $(c\bar{c})_1$ and $(c\bar{c})_0$

Li et al., MPLA29(2014)1450060

The existence of HQSS partners

Cleven et al., PRD92(2015)014005

The status of vector charmonium(-like) states

The status of vector charmonium-like states

- Compact tetraquark

Four states in the mass range 4.22-4.66 GeV

Bhavsar et al., NPA1000(2020)121856

Two states to explain the lineshape

Ali et al., EPJC78(2018)29

- The $D_1\bar{D} + c.c.$ hadronic molecule

Close et al., PRD81(2010)074033

$Y(4230)$ as a $D_1\bar{D} + c.c.$ HM

Ding, PRD79(2009)014001, Wang et al., PRL111(2013)132003

Describe the $D\bar{D}^*\pi$ lineshape

Chen et al., PRD93(2016)014011, Qin et al., PRD94(2016)054035

Three poles $\psi(4160)$, $Y(4230)$, $Y(4320)$

Nakamura et al., 2312.17658

Poles in HQSS

Peng et al., PRD107(2023)016001, Ji et al., PRD129(2022)102002

Two-channel analysis $\psi(4160)$, $Y(4230)$

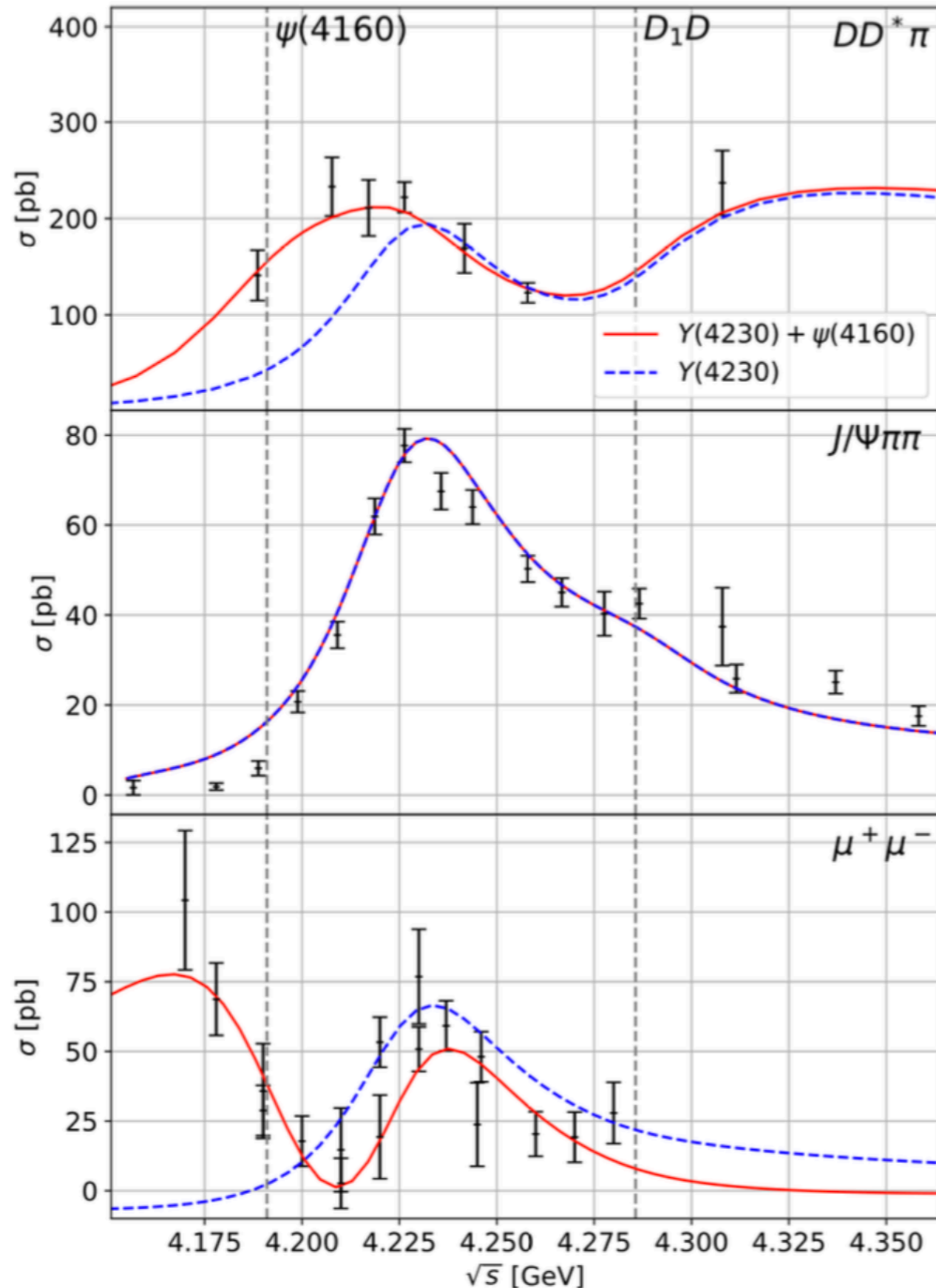
Chen et al., EPJC78(2018)136

Motivation

- **Goal:** eight-channel global fit in the HM picture
- **Disclaimers:**
 - ◆ The interference between $\psi(4160)$ and $Y(4230)$ perturbative
 - ◆ A phenomenological study, uncontrolled uncertainties
 - ◆ Neglect HQSS, i.e. do not consider $D_1\bar{D}^*$, $D_2\bar{D}^*$ channel
 - ◆ Simplified $\pi\pi/K\bar{K}$ FSI [Chen et al., PRD93\(2016\)034030](#), [Chen et al., PRD95\(2017\)034022](#),

[Baru et al., PRD103\(2021\)034016](#), [Molnar et al., PLB797\(2019\)134851](#), [Danilkin et al., PRD102\(2020\)016019](#)

Motivation



- The requirement of $\psi(4160)$
- Describe the $DD^* \pi$ data at lower energy well
- Describe the $e^+ e^- \rightarrow \mu^+ \mu^-$ cross sections well
- Not strong constraint in the $J/\psi \pi \pi$ channel

Detten et al., PRD109(2024)116002

Fit parameters and strategy

- Fitted parameters

	Name	Value
Y	m_Y	(4227 ± 0.4) MeV
	g_{Y0}	$-(10.4 \pm 0.2)$ GeV
	Γ_{in}^Y	(54 ± 1) MeV
	$1/f_Y$	$-(0.012 \pm 0.001)$
	$\delta_{Y\gamma}$	$(17.1 \pm 0.1)^\circ$
ψ	$1/f_\psi$	$-(0.023 \pm 0.003)$
	$\delta_{\psi\gamma}$	$(67 \pm 2)^\circ$
Z_c	m_Z	(3884 ± 1) MeV
	g_{Z0}	(4.15 ± 0.06) GeV
	Γ_{in}^Z	(48 ± 1) MeV
$D\bar{D}^*\pi$	$\alpha_1^{(1)}$	$-(128 \pm 12)$
	$\alpha_2^{(1)}$	$-(3.95 \pm 0.01)$ GeV
	$\beta_1^{(1)}$	$-(202 \pm 18)$
	$\beta_2^{(1)}$	$-(3.89 \pm 0.1)$ GeV
$J/\psi\pi^+\pi^-$	$\alpha_1^{(2)}$	$-(133.9 \pm 4)$
	g_1	$-(14.9 \pm 0.9)10^{-3}$
	g_8	$(24 \pm 1)10^{-3}$
	h_1	$-(16.8 \pm 2.4)10^{-3}$
	h_8	$(15 \pm 0.7)10^{-3}$
	$\beta_1^{(2)}$	(0 ± 0.1)
	c_{CT}^Δ	$-(0.4 \pm 0.1)$ GeV ²
	$f_{J/\psi}$	456 MeV

$\chi_{c0}\omega$	$c_{\chi_{c0}\omega}^\Delta$	(1.469 ± 0.015) GeV ²
	$c_{\chi_{c0}\omega}^Y$	$(0.36 \pm 0.07)10^{-3}$
	$c_{\chi_{c0}\omega}^\psi$	$-(16 \pm 0.5)10^{-3}$
$J/\psi\eta$	$c_{J/\psi\eta}^Y$	$(67.3 \pm 3.4)10^{-3}$ GeV ⁻¹
	$c_{J/\psi\eta}^\psi$	$(298 \pm 11)10^{-3}$ GeV ⁻¹
$X\gamma$	$c_{X\gamma}^Y$	(0.71 ± 0.15) GeV ²
	$c_{X\gamma}^\psi$	(0.017 ± 0.003) GeV
$\mu^+\mu^-$	c_{mix}	(0.6 ± 0.01)

- Fit strategy

① Red parameters fitted in

$$D^0 D^{*-} \pi^+, J/\psi \pi^+ \pi^-, J/\psi K^+ K^-, \mu^+ \mu^-$$

channels

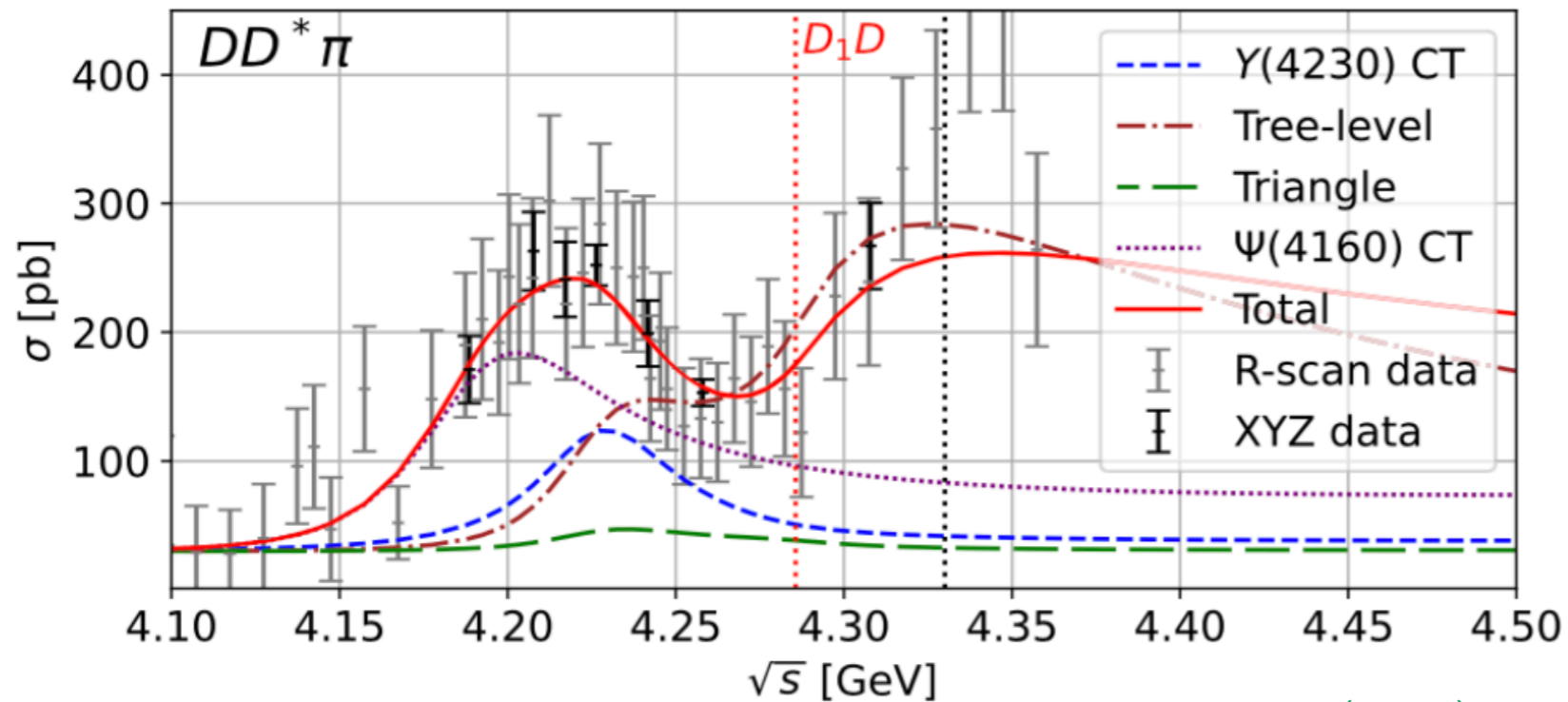
② The remaining parameters are

obtained from the

$$\chi_{c0}\omega, J/\psi\eta, X(3872)\gamma \text{ channels}$$

The $D\bar{D}^*\pi$ channel

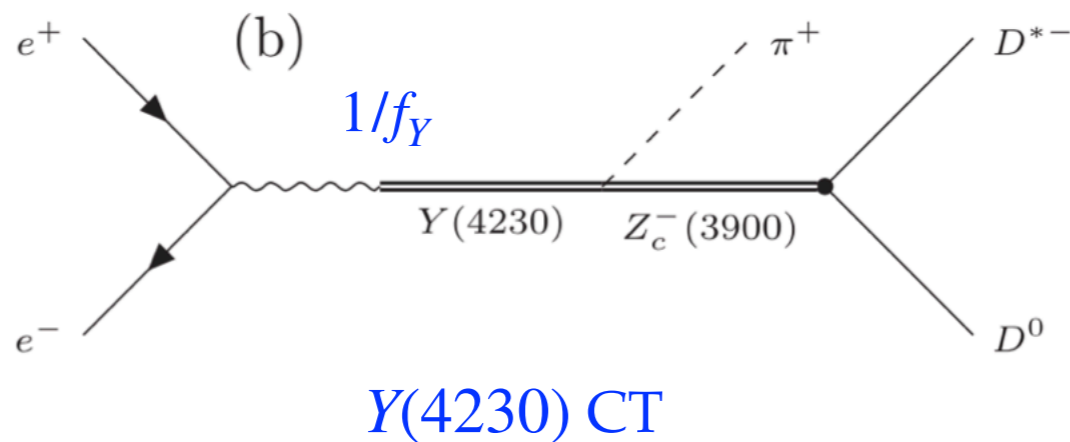
- The $D\bar{D}^*\pi$ lineshape



BESIII, PRL122(2019)102002

- $Y(4230)$ CT

respect
Watson theorem



$$\left(\mathcal{M}_{YCT}^{DD^*\pi}\right)^{kj} = G_Z(E_{DD^*}) g_{Z0} \omega_\pi \left[\alpha_1^{(1)} (\alpha_2^{(1)} + E_{DD^*}) \delta^{kj} \right]$$

$$G_Y(E) = \frac{1}{2\omega_Y} \left(E - m_Y - g_{Y0}^2 \Sigma_{D_1 D}(E) + i\Gamma_{in}^Y/2 \right)^{-1}$$

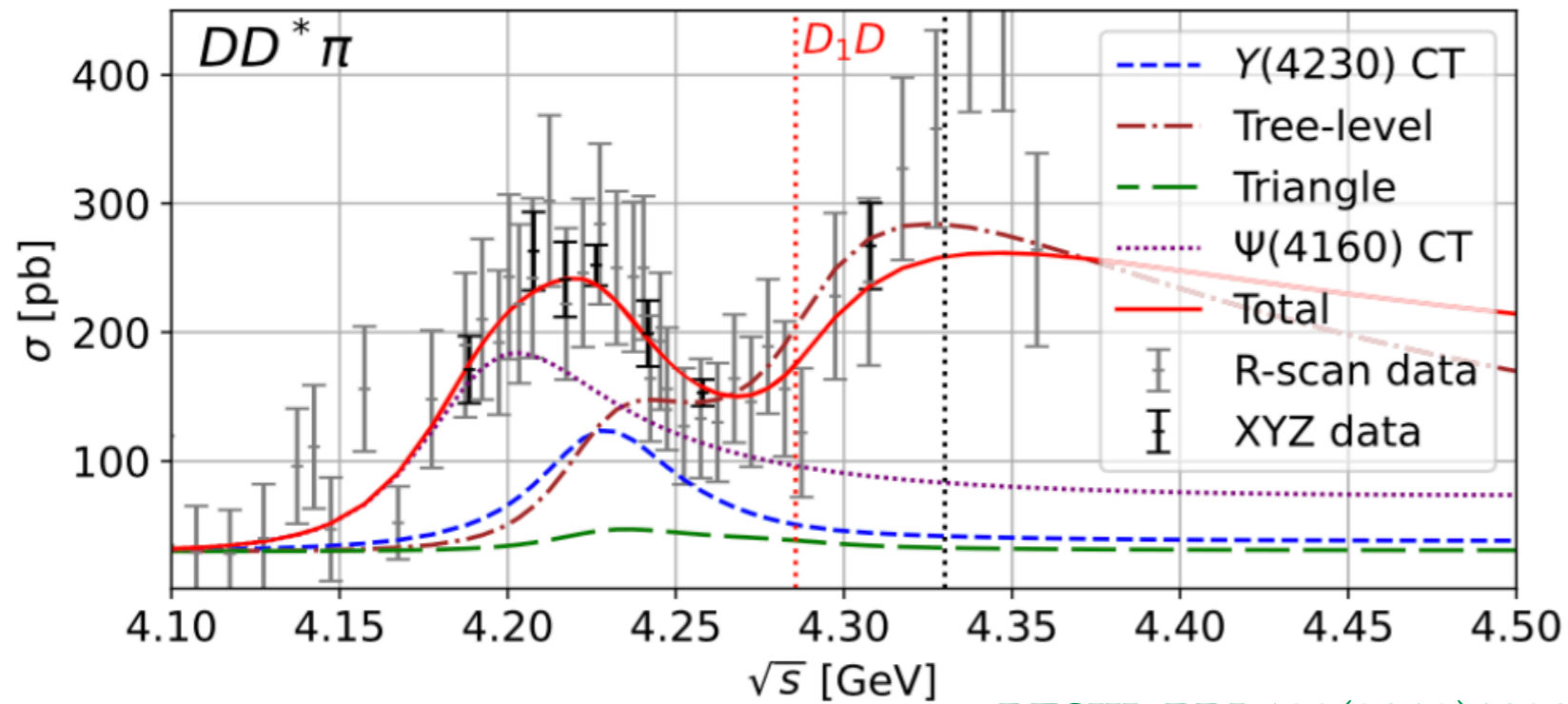
m_Z

g_{Z0}

Γ_{in}^Z

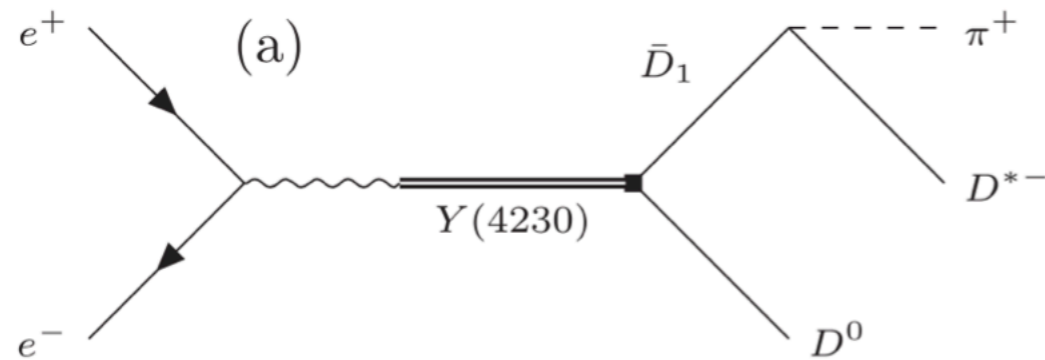
The $D\bar{D}^*\pi$ channel

- The $D\bar{D}^*\pi$ lineshape



BESIII, PRL122(2019)102002

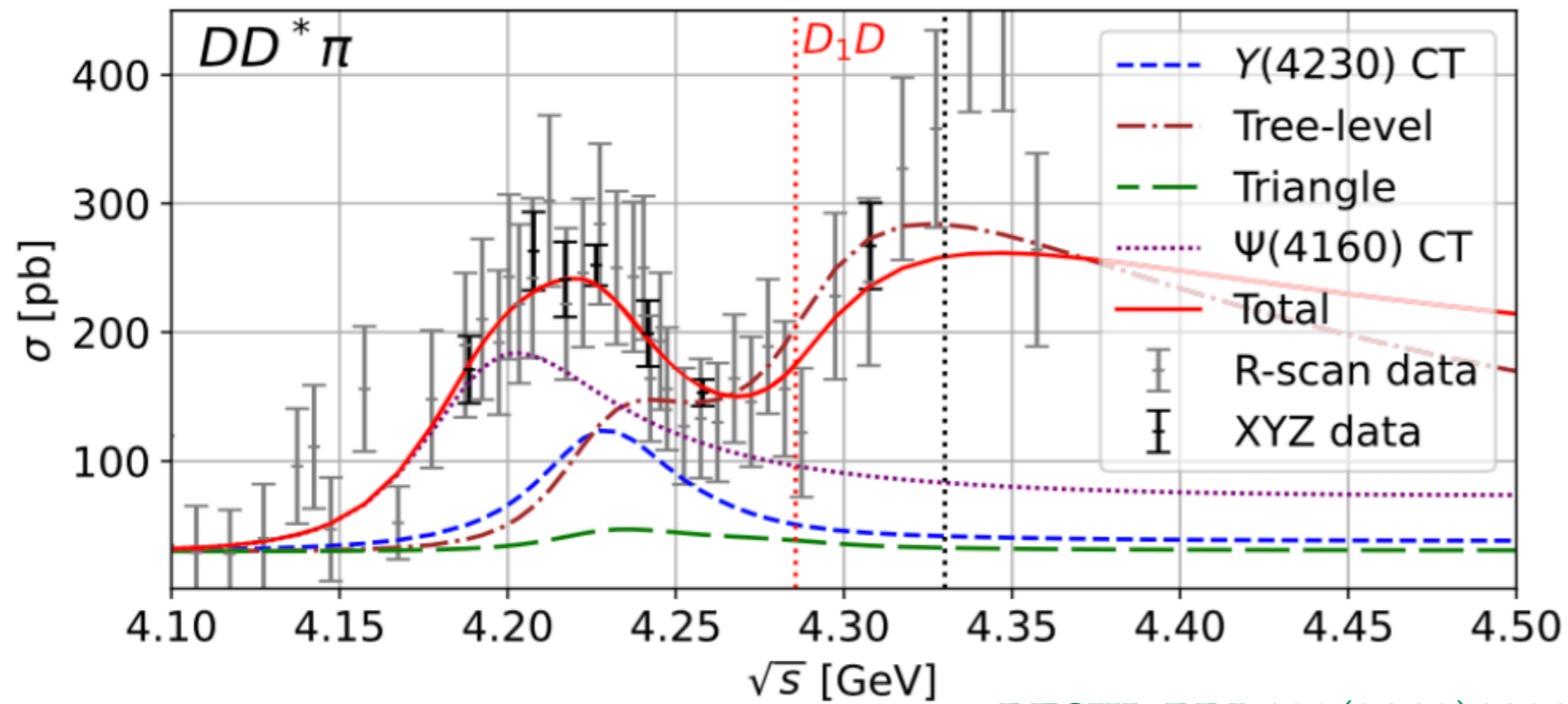
- $Y(4230)$ CT
- D_1 Tree-level



D_1 Tree-level

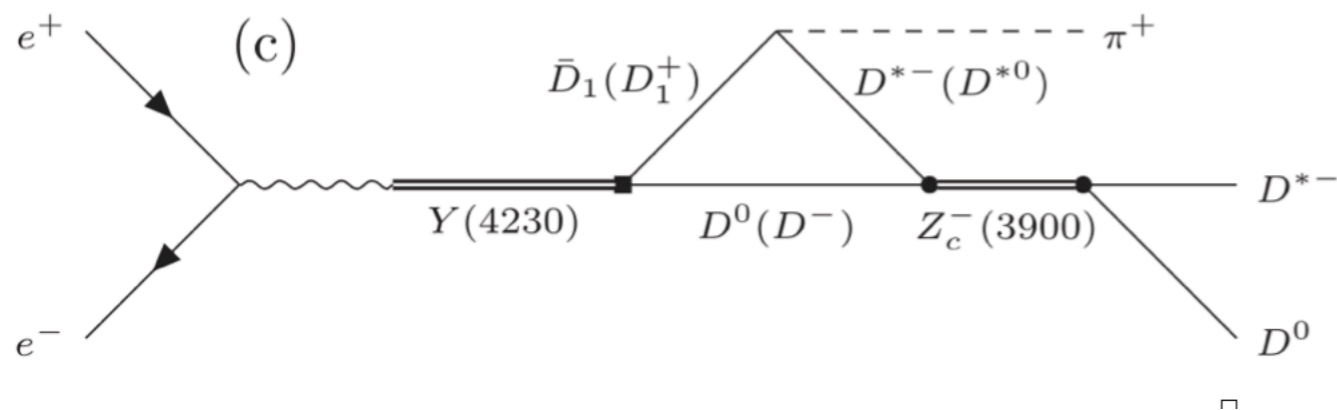
The $D\bar{D}^*\pi$ channel

- The $D\bar{D}^*\pi$ lineshape



BESIII, PRL122(2019)102002

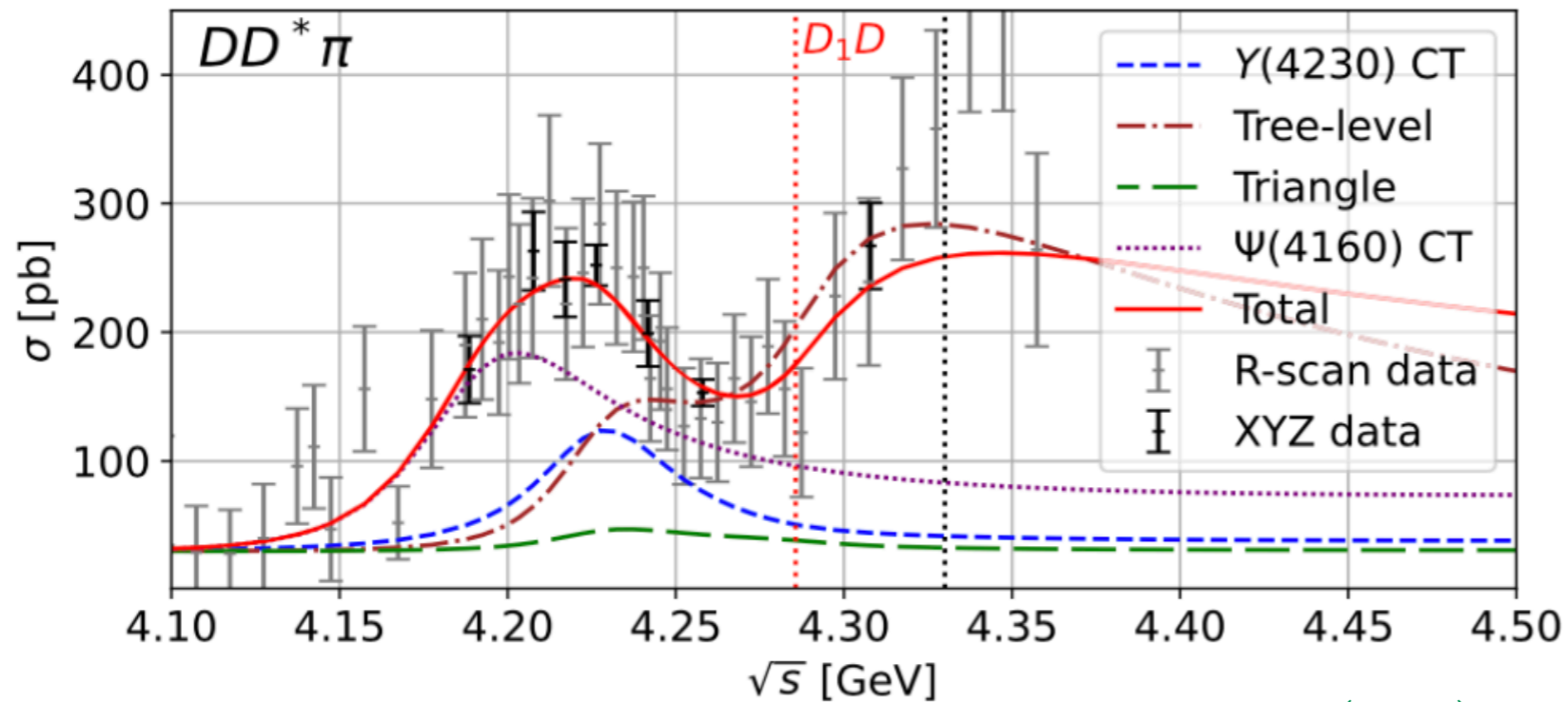
- $Y(4230)$ CT
- D_1 Tree-level
- D_1 Triangle



D_1 Triangle

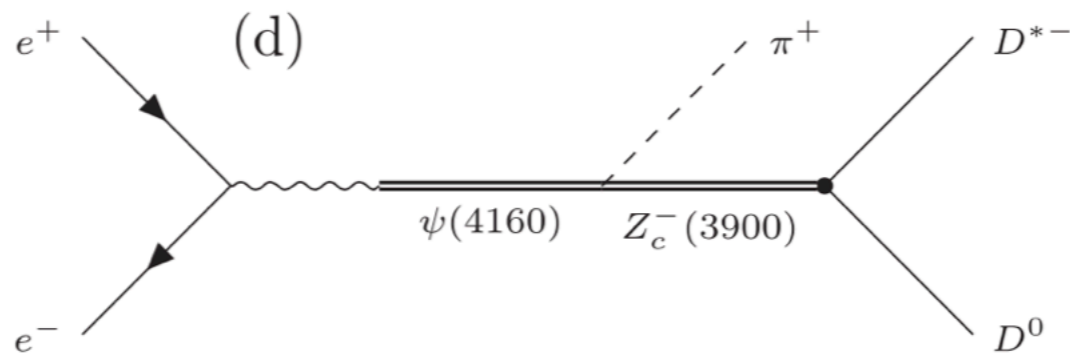
The $D\bar{D}^*\pi$ channel

- The $D\bar{D}^*\pi$ lineshape



BESIII, PRL122(2019)102002

- $Y(4230)$ CT
- D_1 Tree-level
- D_1 Triangle
- $\psi(4160)$ CT

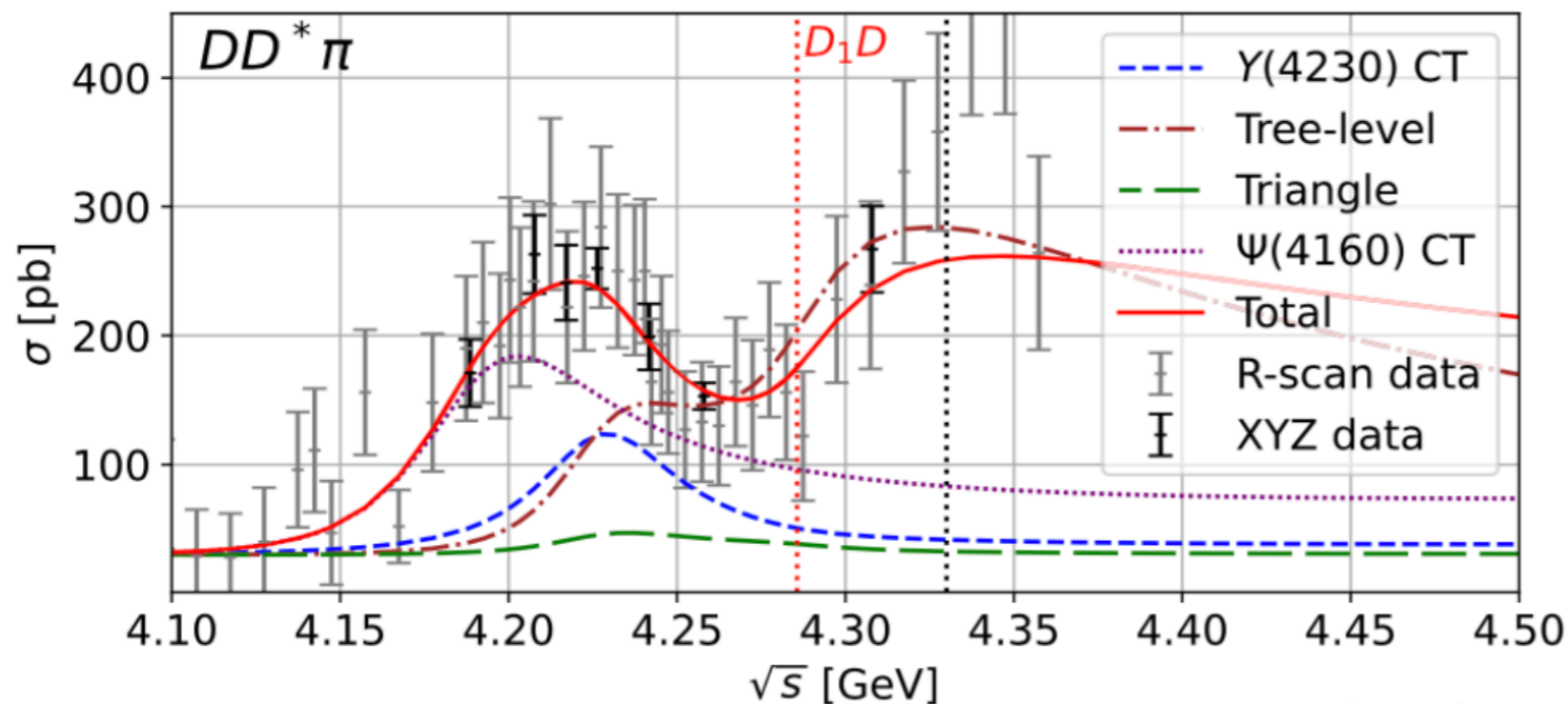


$\psi(4160)$ CT

$$\mathcal{M}_{\psi \rightarrow DD^*\pi}^i = G_\psi g_{Z0} G_Z \omega_\pi \left[\beta_1^{(1)} \left(\beta_2^{(1)} + E_{DD^*} \right) \delta^{ij} \right] \epsilon_{D^*}^{*j}$$

The $D\bar{D}^*\pi$ channel

- The $D\bar{D}^*\pi$ lineshape



BESIII, PRL122(2019)102002

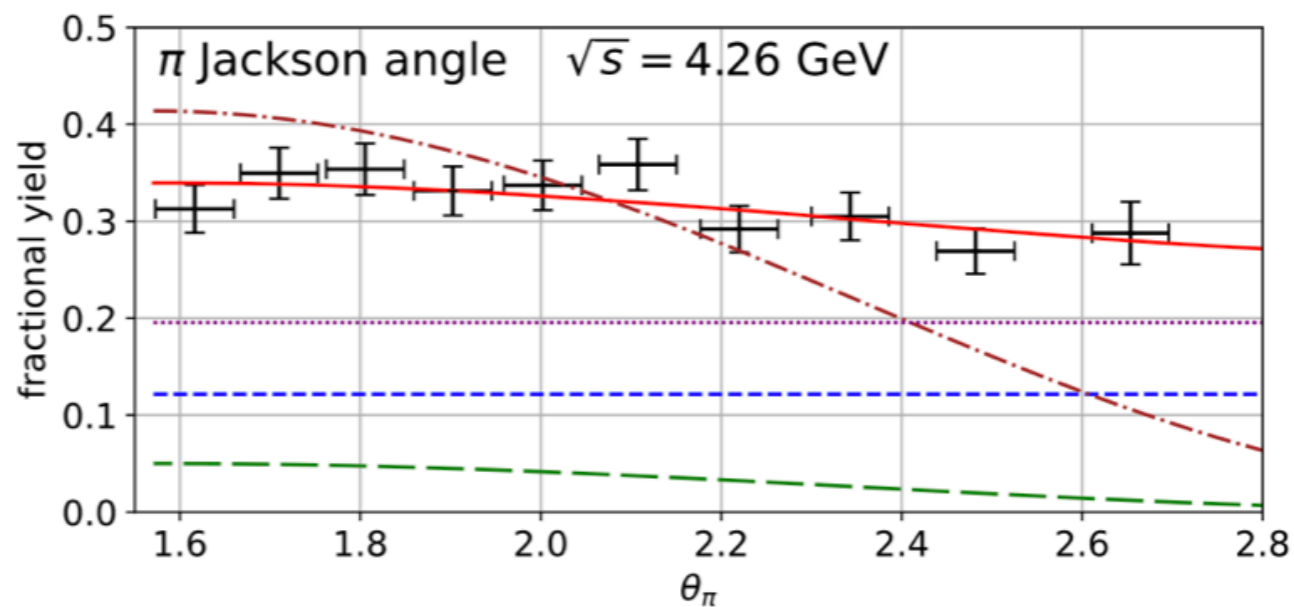
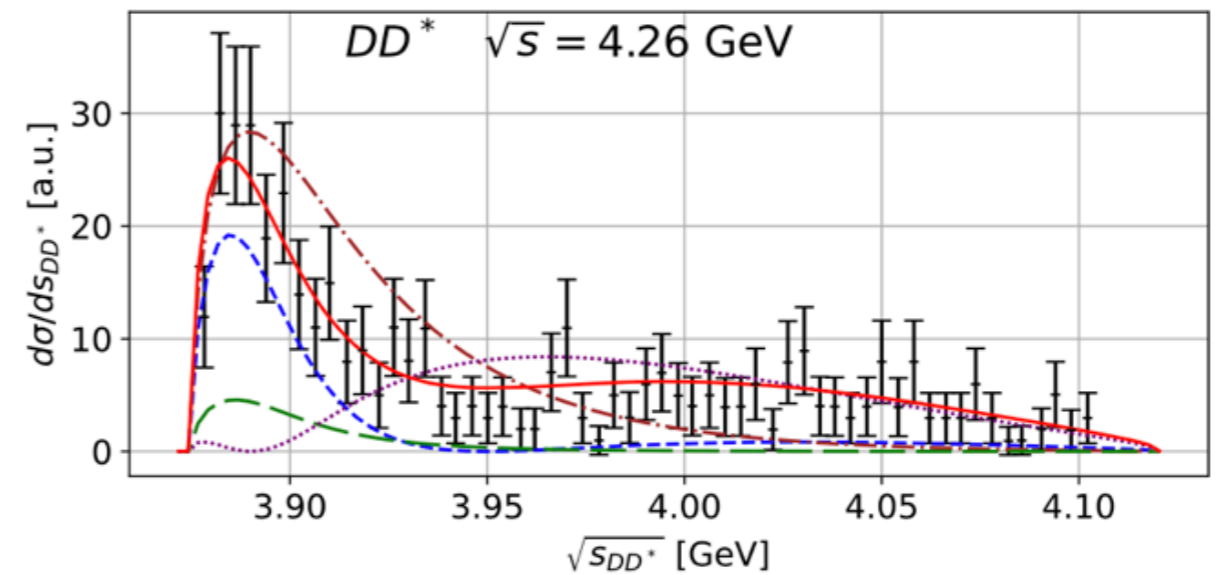
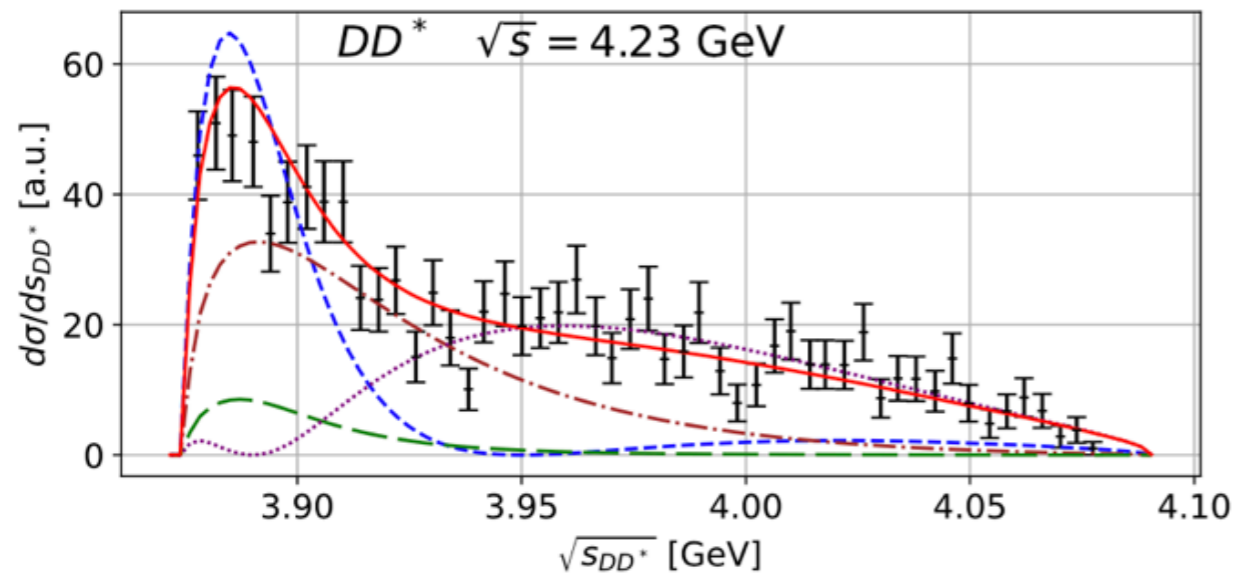
- $Y(4230)$ CT
- D_1 Tree-level
- D_1 Triangle
- $\psi(4160)$ CT

- ① Significant $D_1\bar{D}$ threshold effect from both tree-level and triangle diagrams
- ② Pole of $Y(4230)$ is $(4227 \pm 4) - (25_{-1}^{+4})i$ MeV with uncertainty from the g_{Y_0} , m_0 , Γ_{in} constrained by the $J/\psi\pi\pi$ channel
- ③ Pole of $Z_c(3900)$ is $3884 - 22i$ MeV, higher mass and double width compare to that in

Chen et al., arXiv:2310.15965

The $D\bar{D}^*\pi$ channel

- The subsystem lineshape

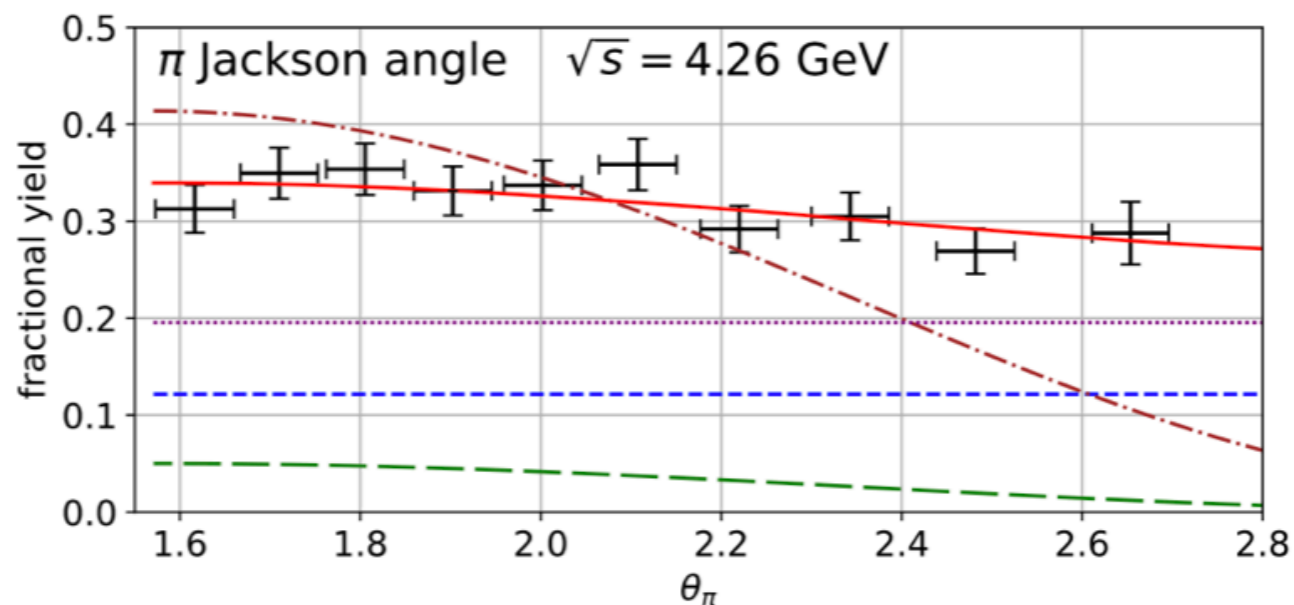
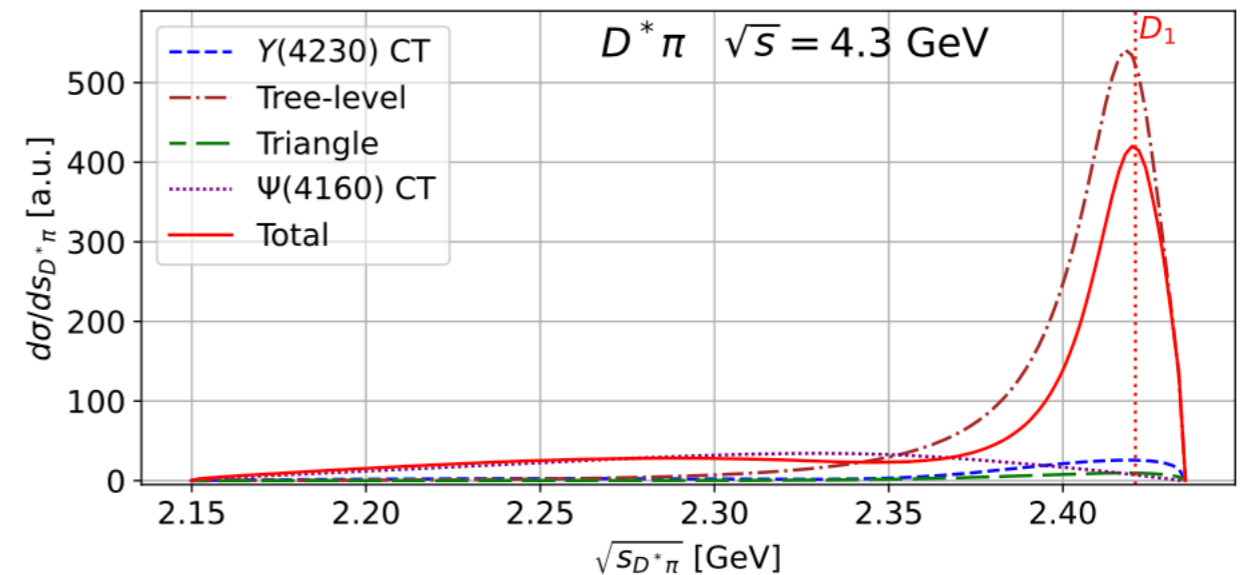
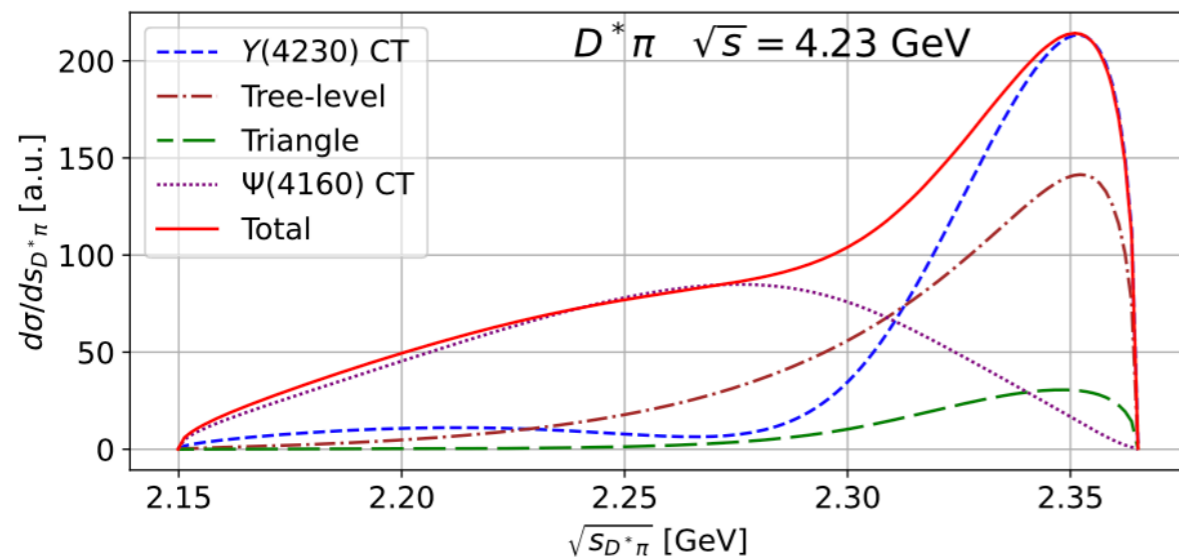


BESIII, PRD92(2015)092006

- ① Constraints from subsystems
- ② Both Z_c and D_1 give enhancement at lower $M_{D\bar{D}^*}$ and higher $M_{\bar{D}^*\pi}$
- ③ The total contribution of D-wave and S-wave give flat pion angular distribution

The $D\bar{D}^*\pi$ channel

- The subsystem lineshape

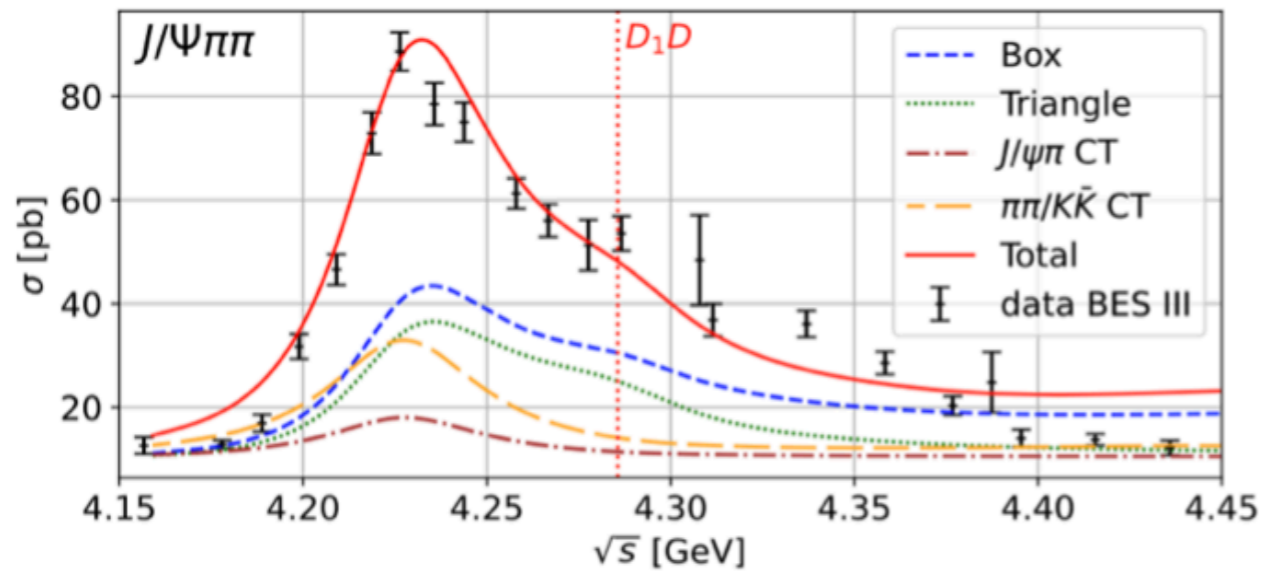


BESIII, PRD92(2015)092006

- ① Constraints from subsystems
- ② Both Z_c and D_1 give enhancement at lower $M_{D\bar{D}^*}$ and higher $M_{\bar{D}^*\pi}$
- ③ The total contribution of D-wave and S-wave give flat pion angular distribution

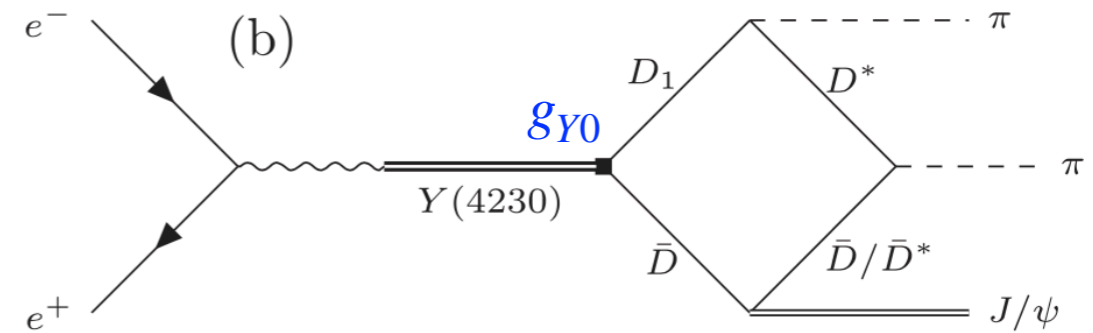
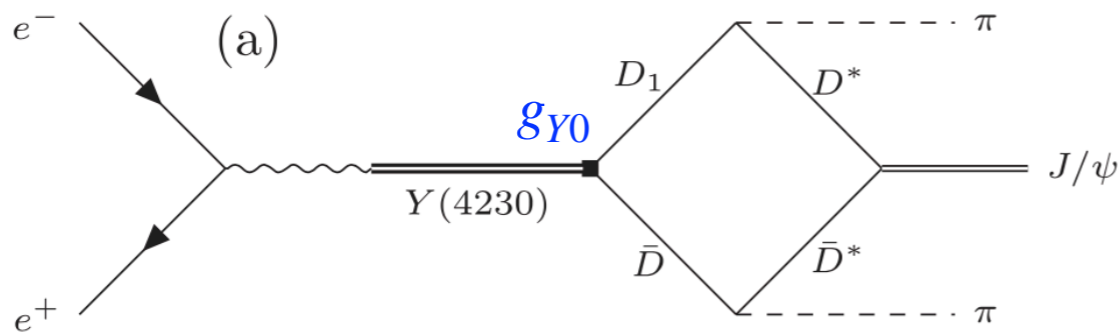
The $J/\psi\pi\pi$ channel

- The $J/\psi\pi\pi$ line shapes



BESIII, PRD106(2022)072001

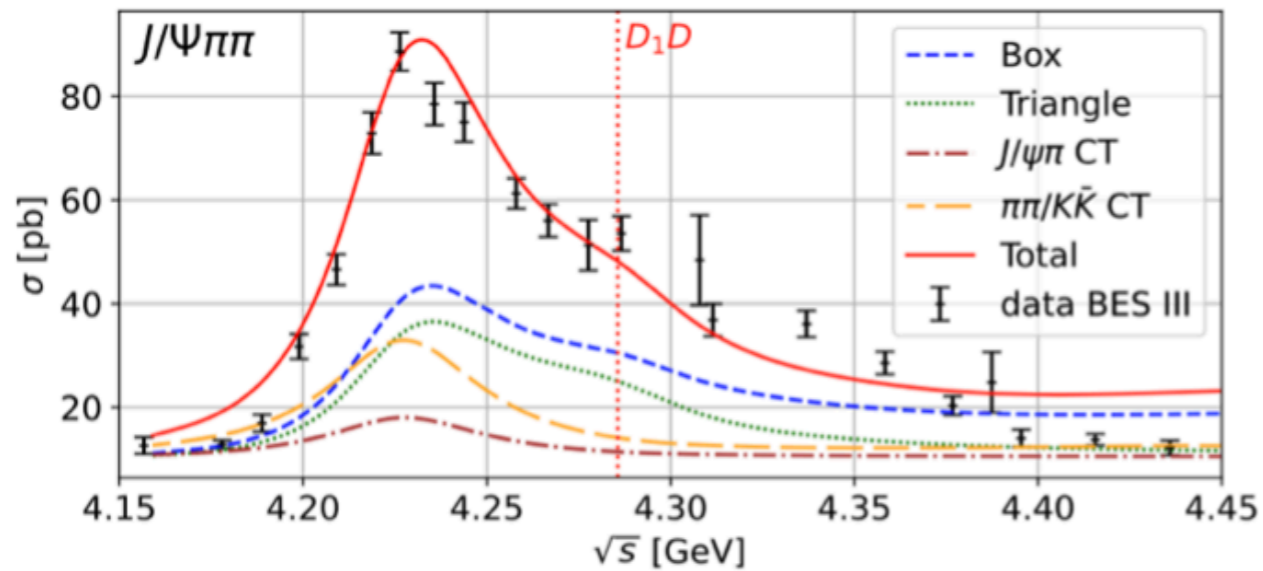
- Box



Box

The $J/\psi\pi\pi$ channel

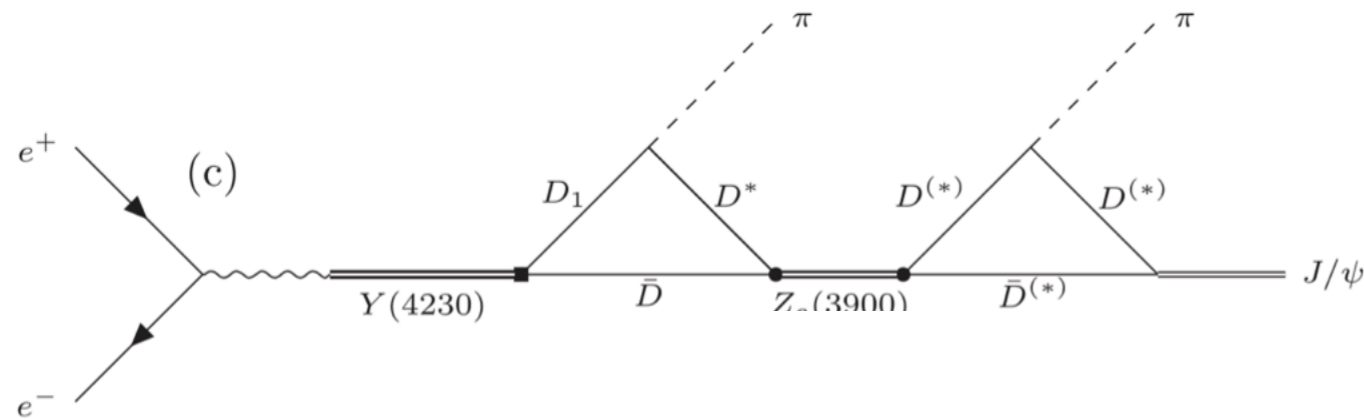
- The $J/\psi\pi\pi$ line shapes



BESIII, PRD106(2022)072001

• Box

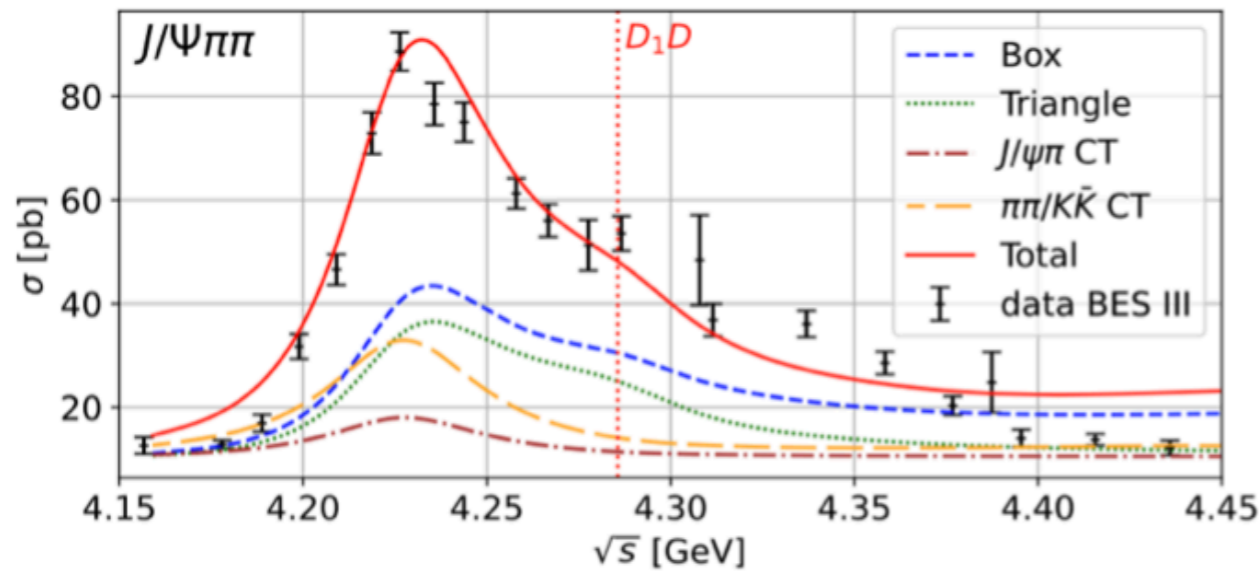
• Triangle



Triangle

The $J/\psi\pi\pi$ channel

- The $J/\psi\pi\pi$ line shapes

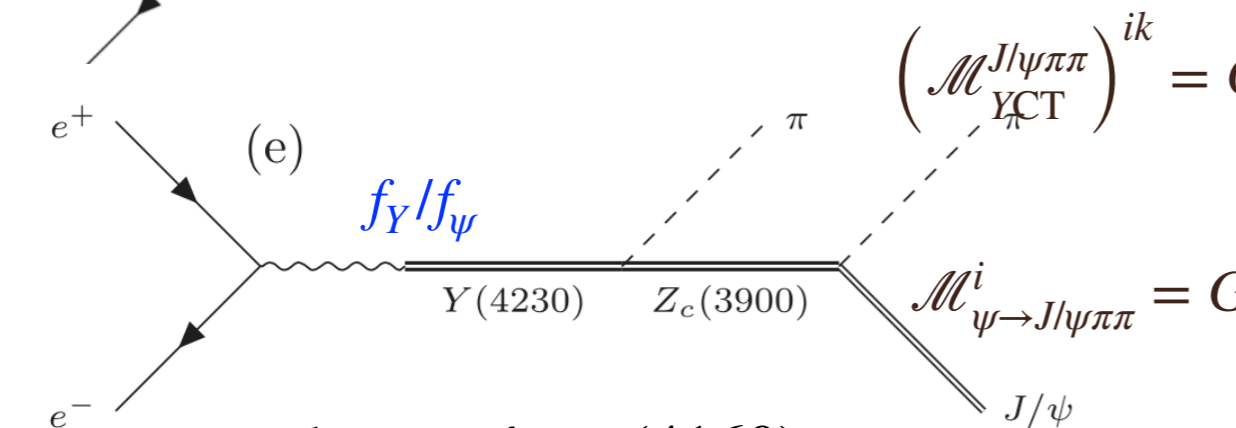
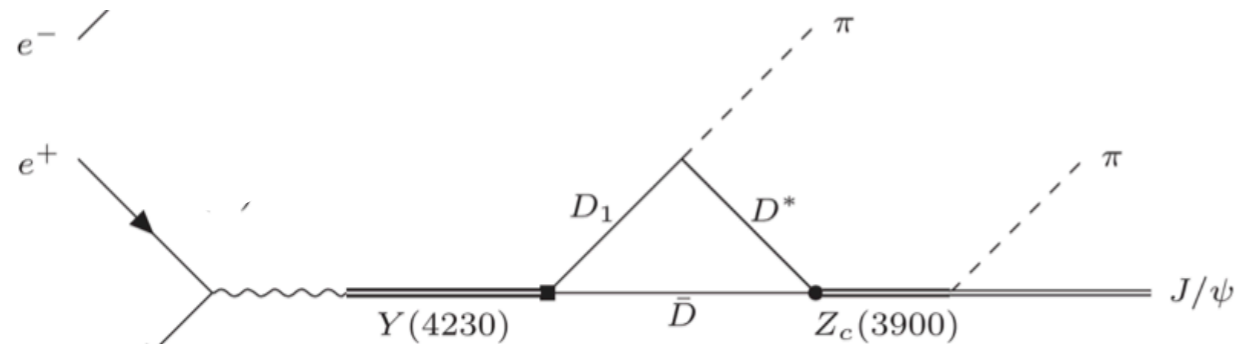


BESIII, PRD106(2022)072001

- Box
- Triangle
- $J/\psi\pi$ CT

$J/\psi\pi$ CT

$$g_{J/\psi\pi}^{Z_c ik} = g_{Z_0} \left(\mathcal{M}_2^\Delta \right)^{ik} + \omega_{\pi_2} c_{CT}^\Delta \delta^{ik}$$



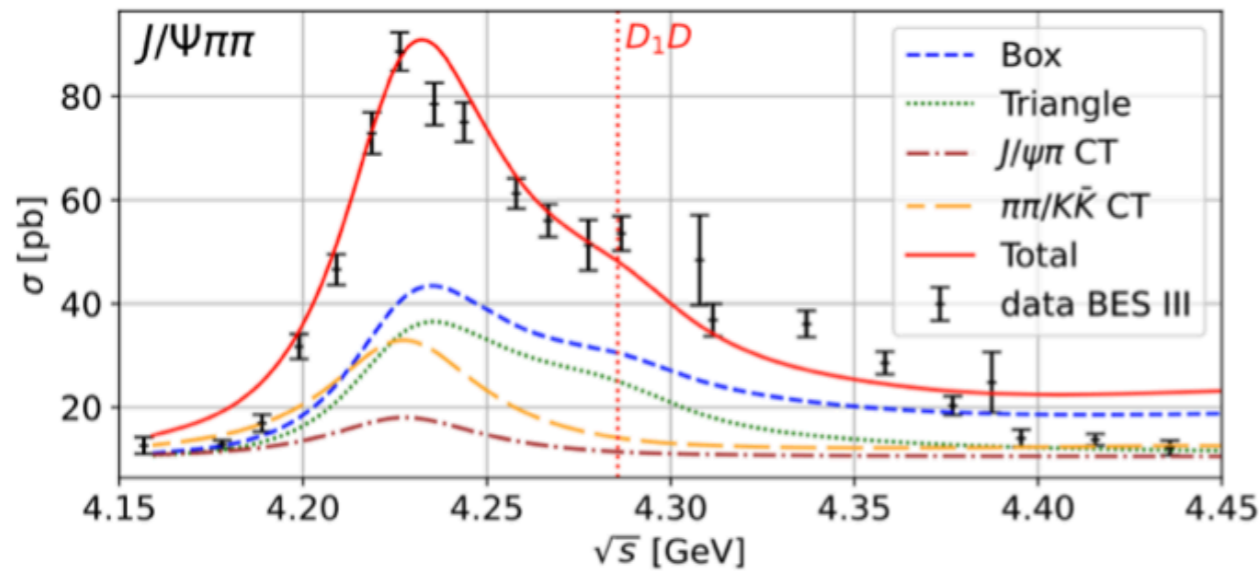
Analogous for $\psi(4160)$

$$\left(\mathcal{M}_{YCT}^{J/\psi\pi\pi} \right)^{ik} = G_Z g_{J/\psi\pi}^{Zik} \omega_{\pi_1} \left[\alpha_1^{(2)} \left(\alpha_2^{(2)} + E_{J/\psi\pi} \right) \right] + \Omega_{11} M_0^{\pi\pi} + \frac{2}{\sqrt{3}} \Omega_{12} M_0^{KK}$$

$$\mathcal{M}_{\psi \rightarrow J/\psi\pi\pi}^i = G_\psi \left[\beta_1^{(2)} \left(\beta_2^{(2)} + E_{J/\psi\pi_1} \right) \right] g_{J/\psi\pi}^{Zil} \omega_{\pi_1} G_Z \left(E_{J/\psi\pi_1} \right) \epsilon_{J/\psi}^{*l} + \left(p_{\pi_1} \leftrightarrow p_{\pi_2} \right)$$

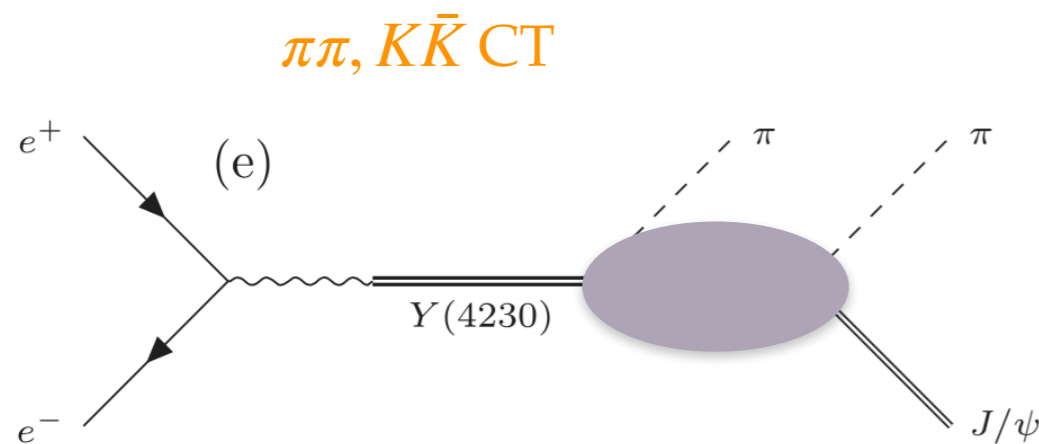
The $J/\psi\pi\pi$ channel

- The $J/\psi\pi\pi$ line shapes



BESIII, PRD106(2022)072001

- Box
- Triangle
- $J/\psi\pi$ CT
- $\pi\pi, K\bar{K}$ CT



$$\mathcal{L}_{Y\psi\phi\phi} = g_1 \langle V_1^\alpha J_\alpha^\dagger \rangle \langle u_\mu u^\mu \rangle + h_1 \langle V_1^\alpha J_\alpha^\dagger \rangle \langle u_\mu u_\nu \rangle v^\mu v^\nu$$

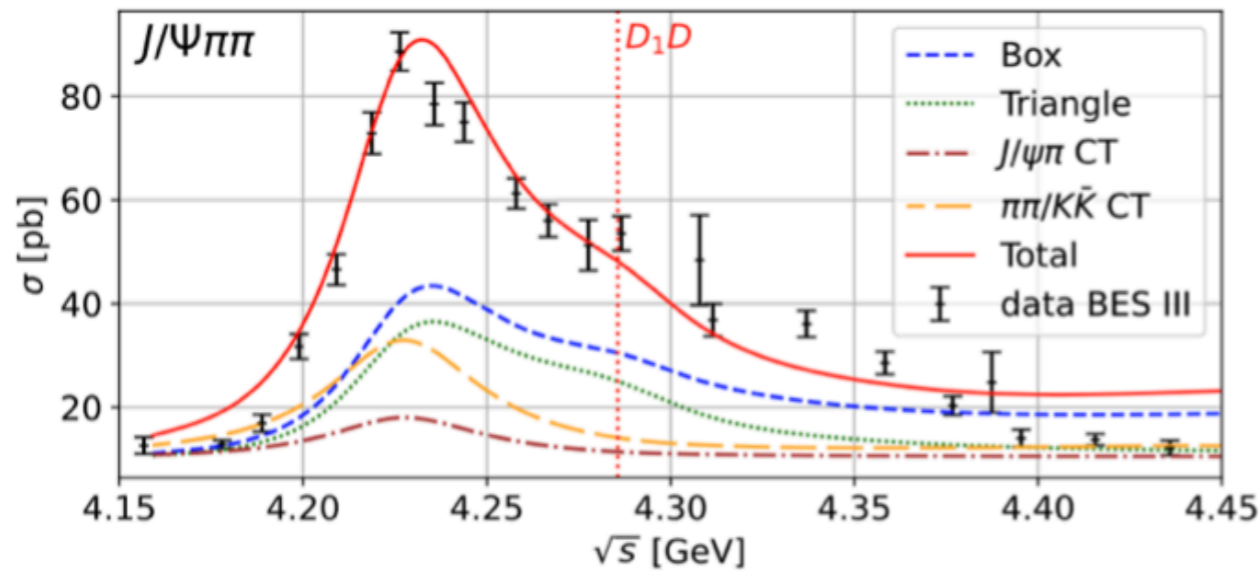
$$+ g_8 \langle J_\alpha^\dagger \rangle \langle V_8^\alpha u_\mu u^\mu \rangle + h_8 \langle J_\alpha^\dagger \rangle \langle V_8^\alpha u_\mu u_\nu \rangle v^\mu v^\nu + \text{H.c.}$$

Isken et al., EPJC77(2017)489

$$\left(\mathcal{M}_{YCT}^{J/\psi\pi\pi} \right)^{ik} = G_Z g_{J/\psi\pi}^{Zik} \omega_{\pi_1} \left[\alpha_1^{(2)} \left(\alpha_2^{(2)} + E_{J/\psi\pi} \right) \right] + \Omega_{11} M_0^{\pi\pi} + \frac{2}{\sqrt{3}} \Omega_{12} M_0^{KK}$$

The $J/\psi\pi\pi$ channel

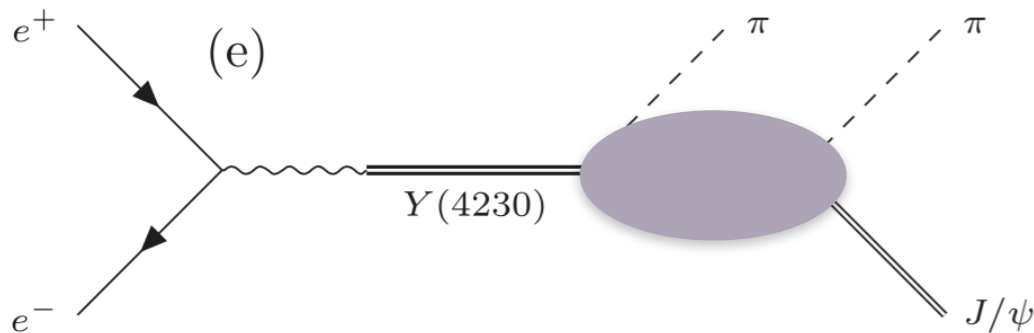
- The $J/\psi\pi\pi$ line shapes



BESIII, PRD106(2022)072001

- Box
- Triangle
- $J/\psi\pi$ CT
- $\pi\pi, K\bar{K}$ CT

$\pi\pi, K\bar{K}$ CT

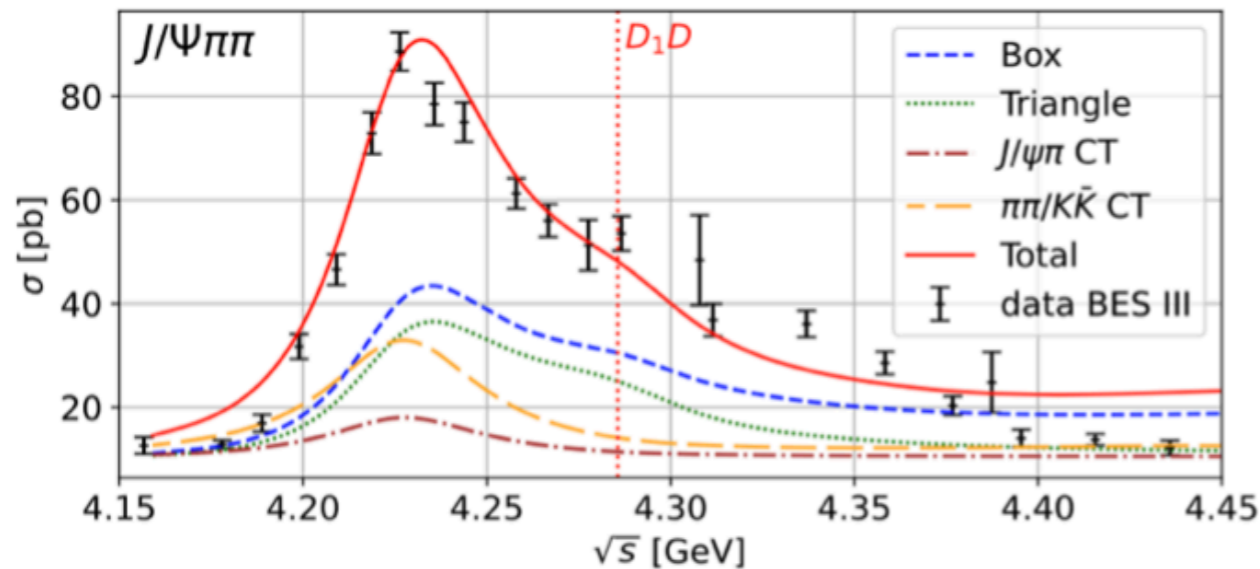


$$M_0^{\pi\pi} = -\frac{2}{f^2} \sqrt{m_Y m_{J/\psi}} \left(g_1 + \frac{g_8}{\sqrt{2}} \right) (s - 2m_\pi^2) + \frac{h_1 + \frac{h_8}{\sqrt{2}}}{2} \left[s + q^2 \left(1 - \frac{\sigma_\pi}{3} \right) \right]$$

$$\left(\mathcal{M}_{YCT}^{J/\psi\pi\pi} \right)^{ik} = G_Z g_{J/\psi\pi}^{Zik} \omega_{\pi_1} \left[\alpha_1^{(2)} \left(\alpha_2^{(2)} + E_{J/\psi\pi} \right) \right] + \Omega_{11} M_0^{\pi\pi} + \frac{2}{\sqrt{3}} \Omega_{12} M_0^{KK}$$

The $J/\psi\pi\pi$ channel

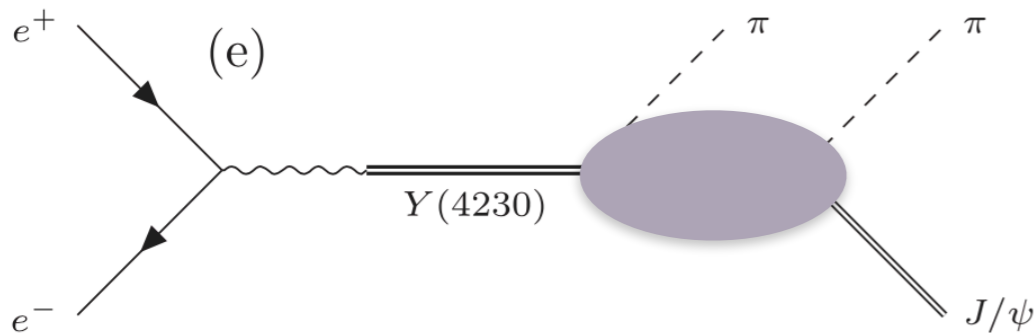
- The $J/\psi\pi\pi$ line shapes



BESIII, PRD106(2022)072001

- Box
- Triangle
- $J/\psi\pi$ CT
- $\pi\pi, K\bar{K}$ CT

$\pi\pi, K\bar{K}$ CT

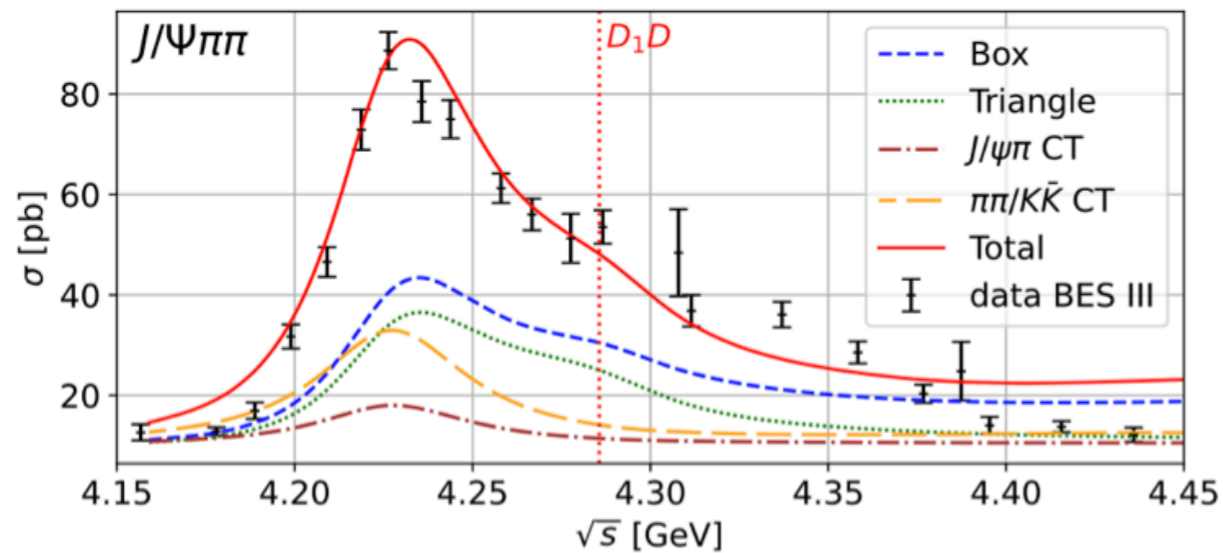
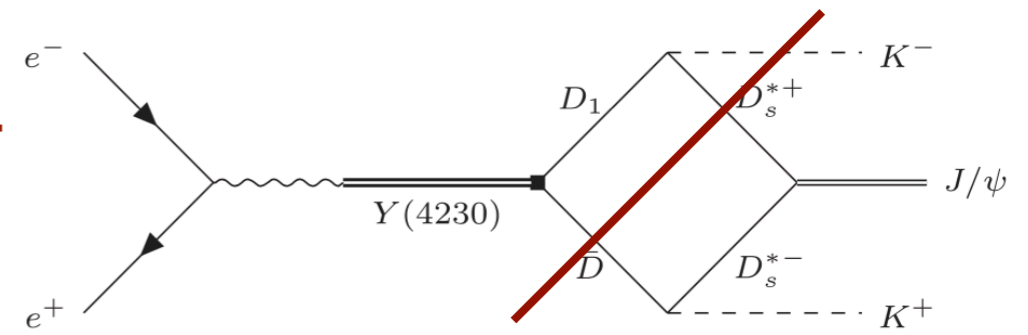


$$M_0^{KK} = -\frac{2}{f^2} \sqrt{m_Y m_{J/\psi}} \left(g_1 - \frac{g_8}{2\sqrt{2}} \right) (s - 2m_K^2) + \frac{h_1 - \frac{h_8}{2\sqrt{2}}}{2} \left[s + q^2 \left(1 - \frac{\sigma_K}{3} \right) \right]$$

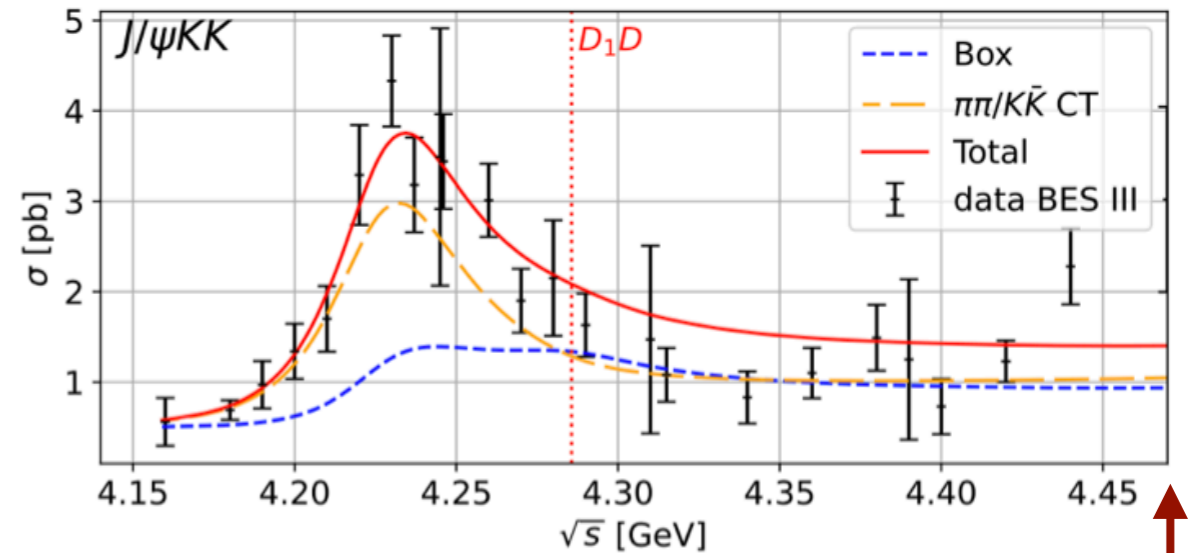
$$\left(\mathcal{M}_{YCT}^{J/\psi\pi\pi} \right)^{ik} = G_Z g_{J/\psi\pi}^{Zik} \omega_{\pi_1} \left[\alpha_1^{(2)} \left(\alpha_2^{(2)} + E_{J/\psi\pi} \right) \right] + \Omega_{11} M_0^{\pi\pi} + \frac{2}{\sqrt{3}} \Omega_{12} M_0^{KK}$$

The $J/\psi\pi\pi$, $J/\psi K\bar{K}$ channels

- The $J/\psi\pi\pi$, $J/\psi K\bar{K}$ line shapes



BESIII, PRD106(2022)072001



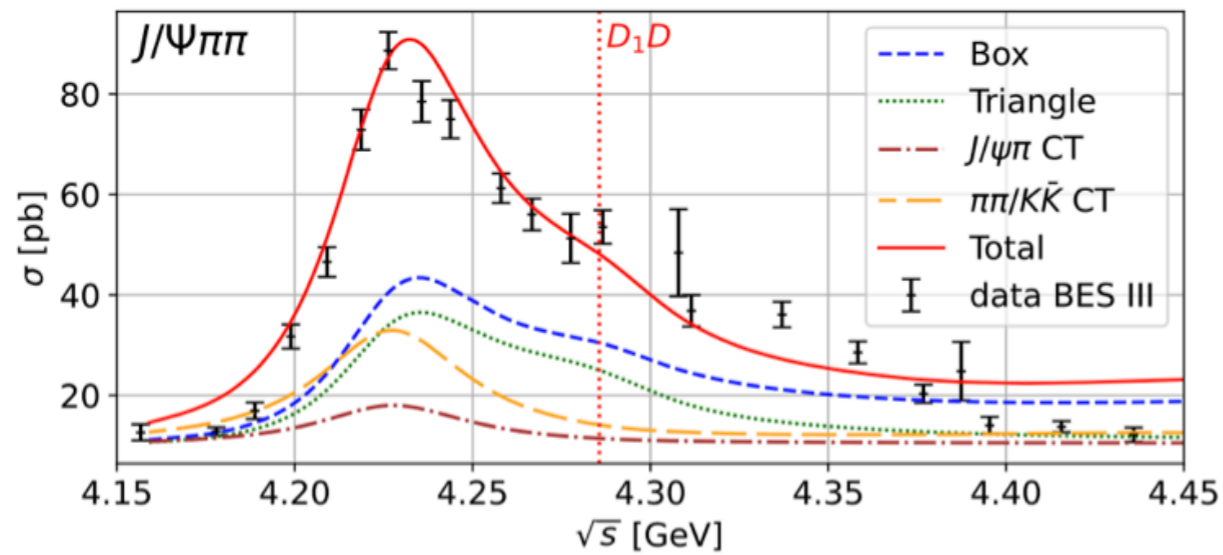
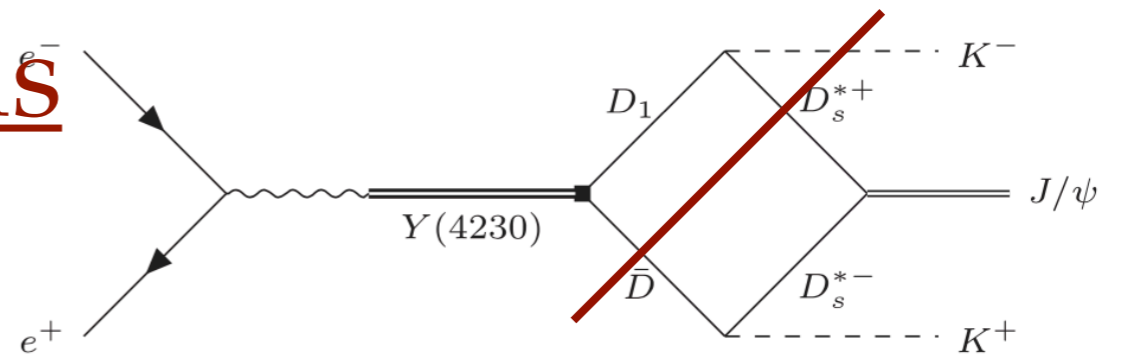
BESIII, CPC46(2022)111002

$D_s^{*+} \bar{D} K^-$

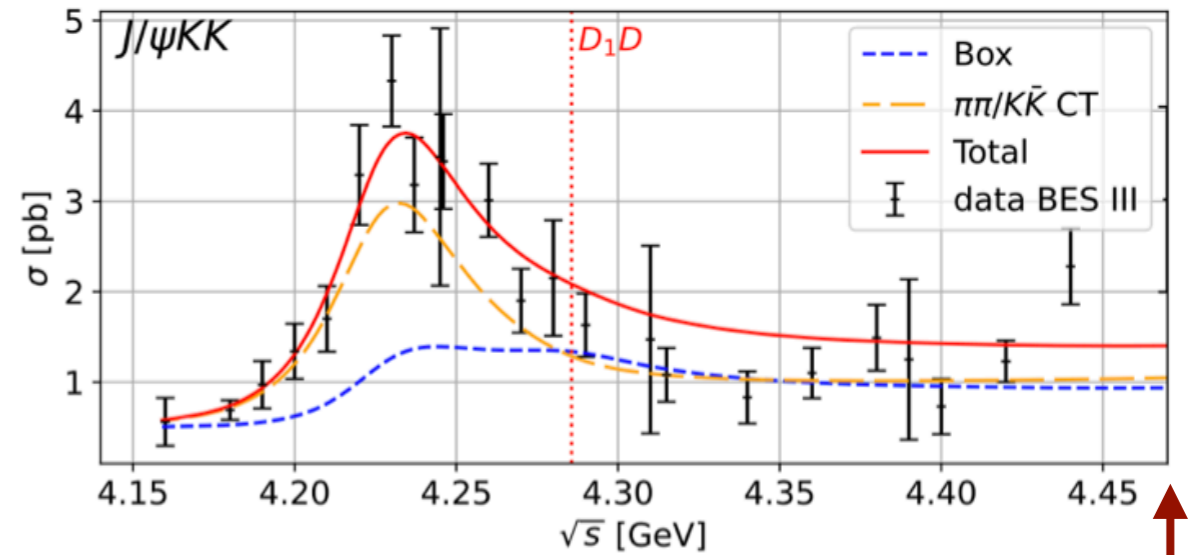
- ① Asymmetric lineshape from $D_1 \bar{D}$ threshold, i.e. Box and Triangle
- ② Strange source, but no $Z_{cS'}$ for $J/\psi K\bar{K}$ channel
- ③ The leading effect is driven by the $\pi\pi/K\bar{K}$ FSI for the $J/\psi K\bar{K}$ channel
- ④ Energy goes beyond the $D_s^{*+} \bar{D} K^-$ threshold, the strange source is important
- ⑤ Describe the lineshape of the subsystems

The $J/\psi\pi\pi, J/\psi K\bar{K}$ channels

- The $J/\psi\pi\pi, J/\psi K\bar{K}$ line shapes

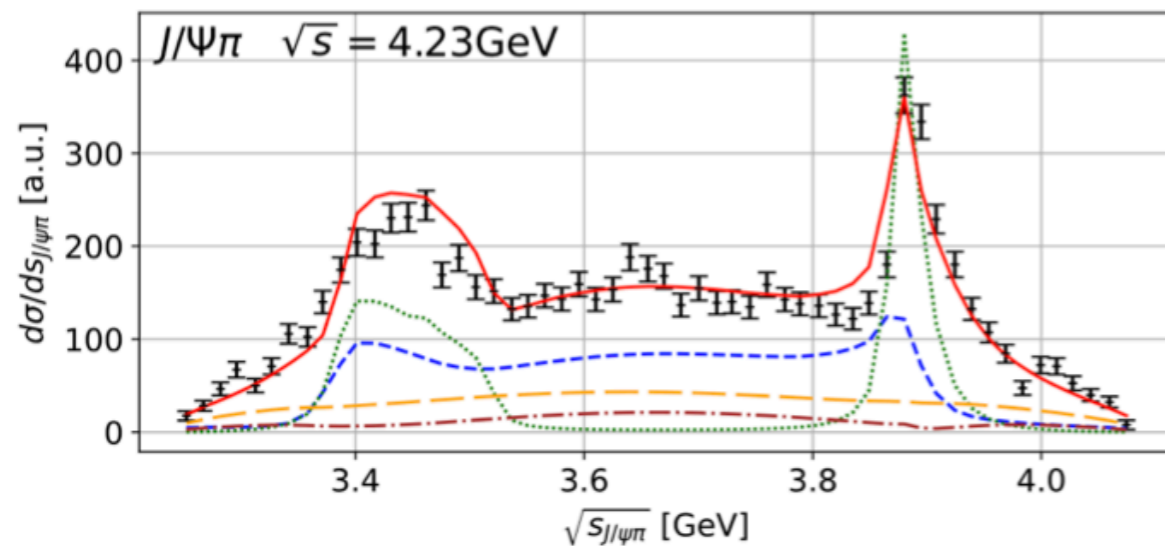


BESIII, PRD106(2022)072001

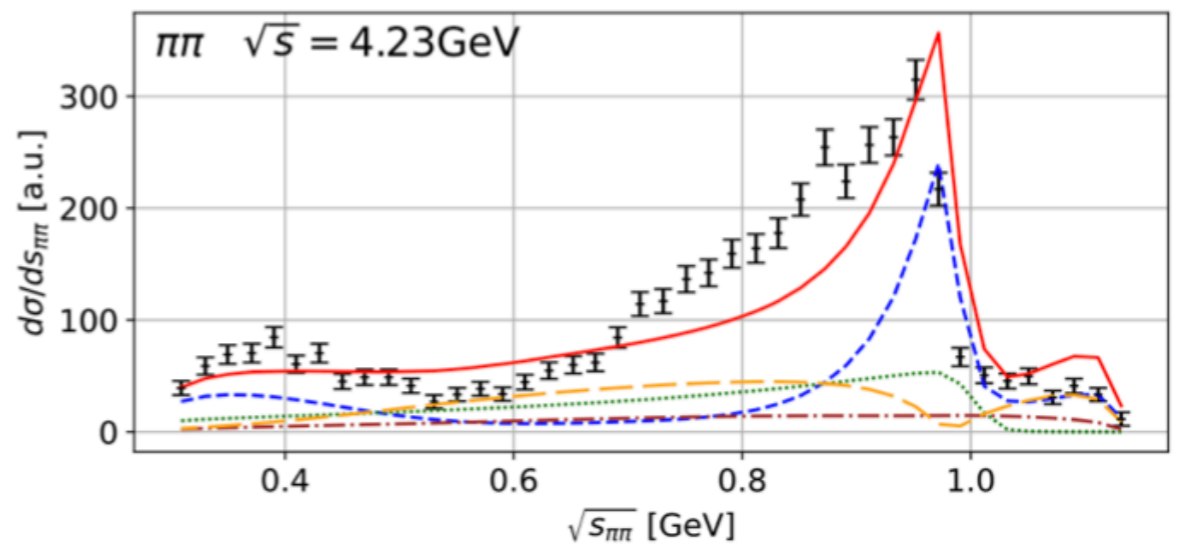


BESIII, CPC46(2022)111002

$D_s^{*+} \bar{D} K^-$

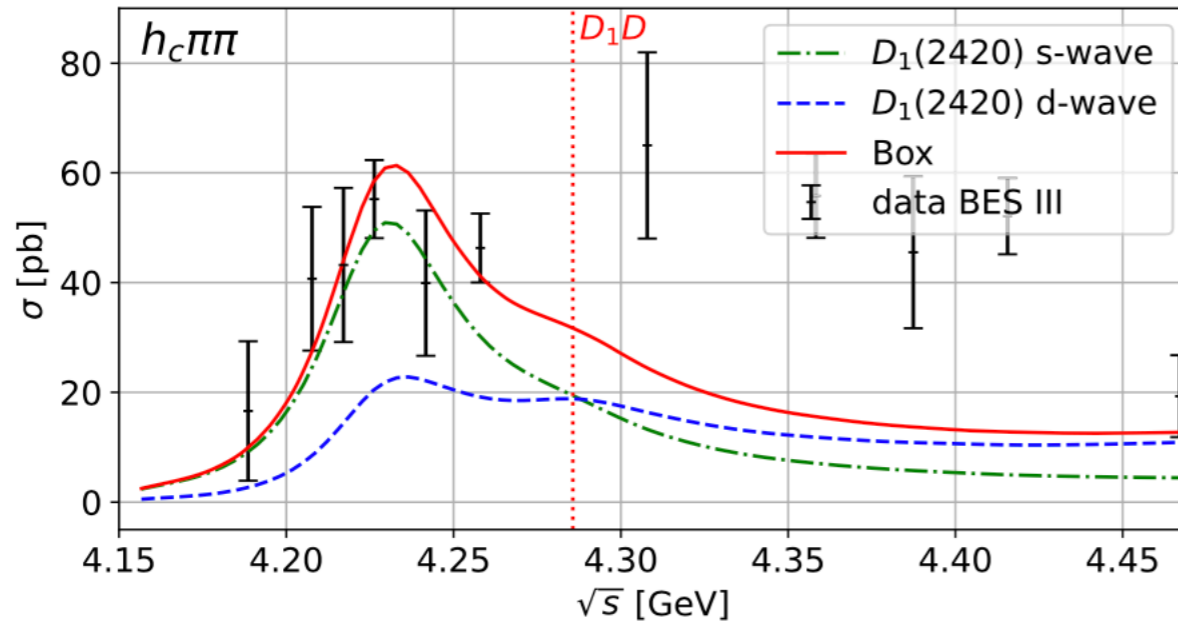


BESIII, PRL119(2017)072001



The $h_c \pi \pi$ channel

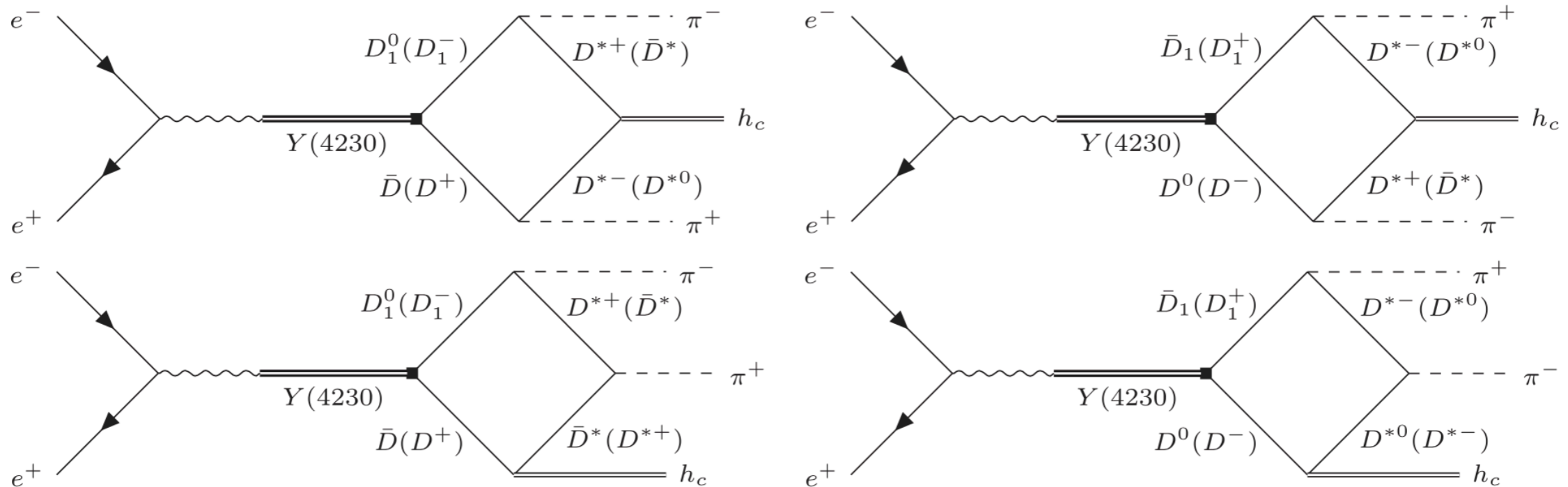
- The $h_c \pi \pi$ line shapes



• D-wave D_1

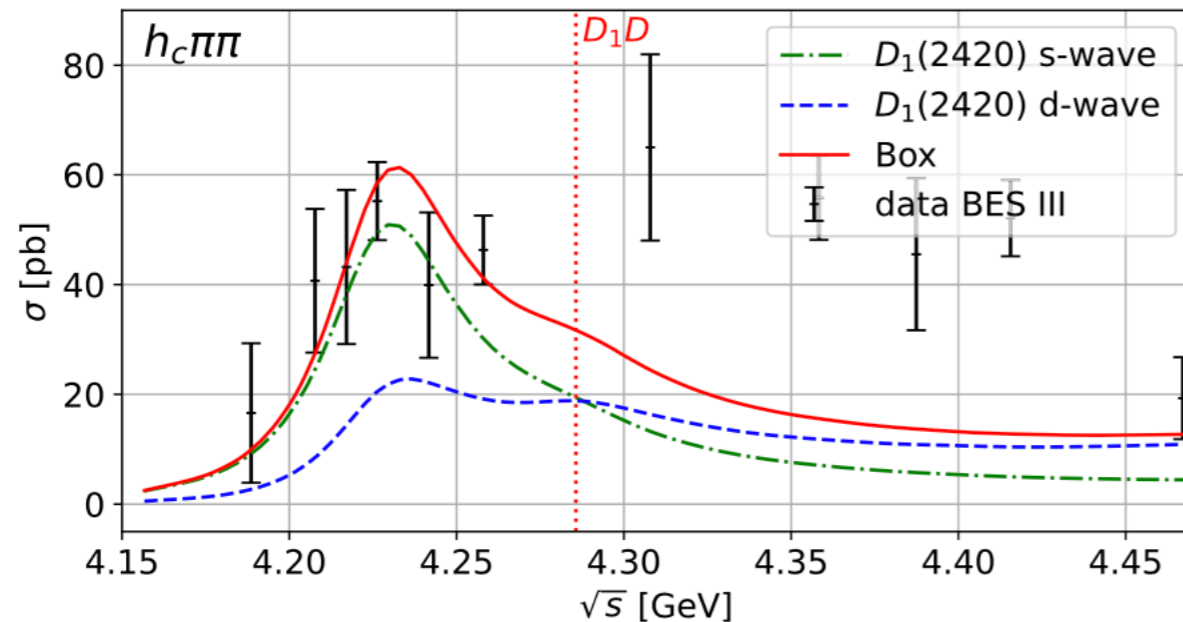
• S-wave D_1

BESIII, PRL118(2017)092002



The $h_c\pi\pi$ channel

- The $h_c\pi\pi$ line shapes



• D-wave D_1

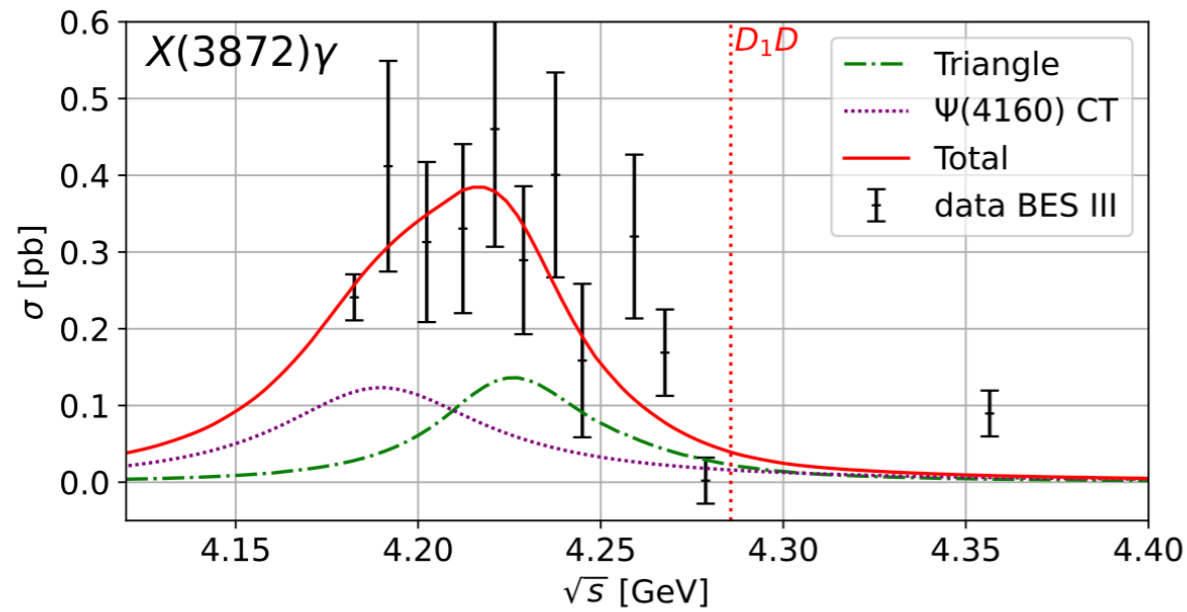
• S-wave D_1

BESIII, PRL118(2017)092002

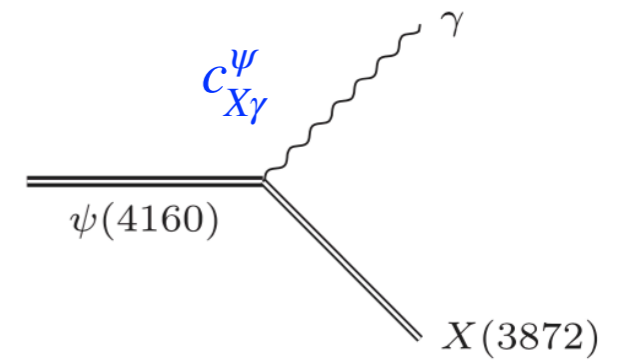
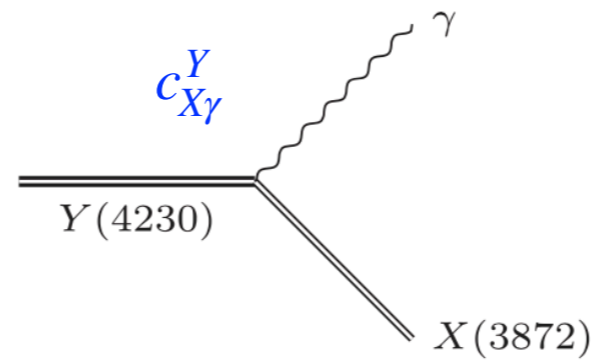
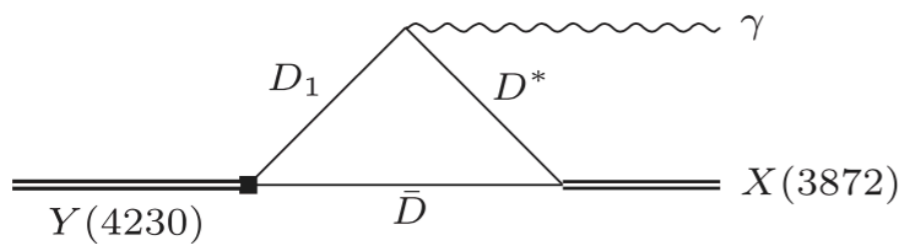
- ① No $Z_c(3900)$ observed in $h_c\pi$ channel, only consider box diagram
- ② No S-wave $\pi\pi$ FSI
- ③ Cross section is with the same order as that of the $J/\psi\pi\pi$ channel
- ④ Large HQSS violation is accepted in HM picture naturally

The $J/\psi\eta$, $\chi_{c0}\omega$, $X(3872)\gamma$ channels

- The $J/\psi\eta$, $\chi_{c0}\omega$, $X(3872)\gamma$ line shapes

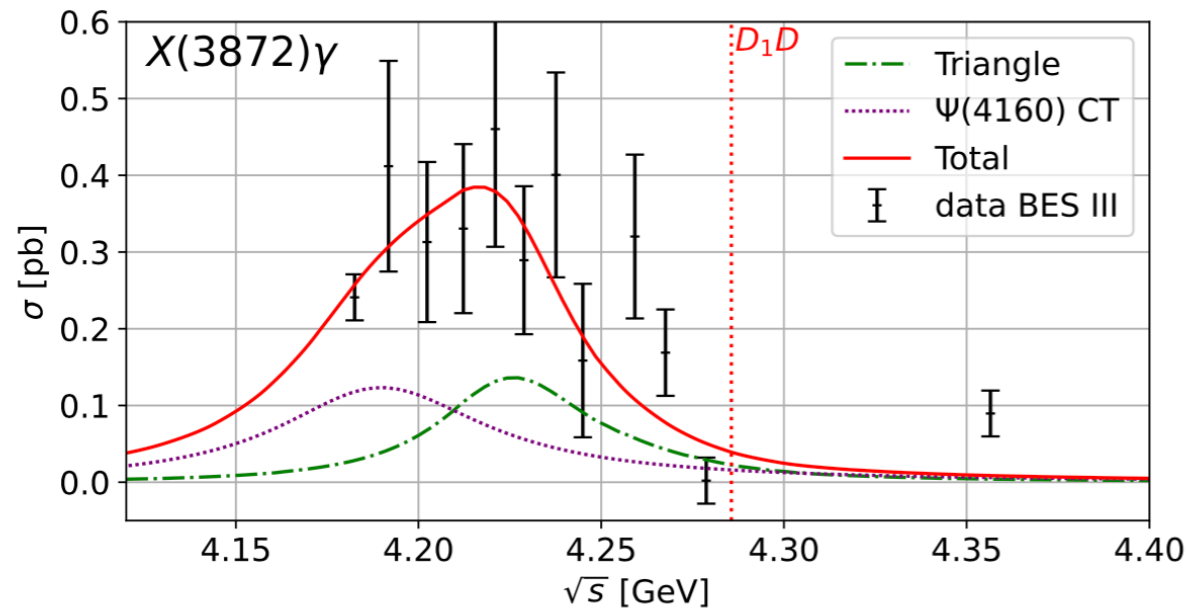


BESIII, PRL122(2019)232002

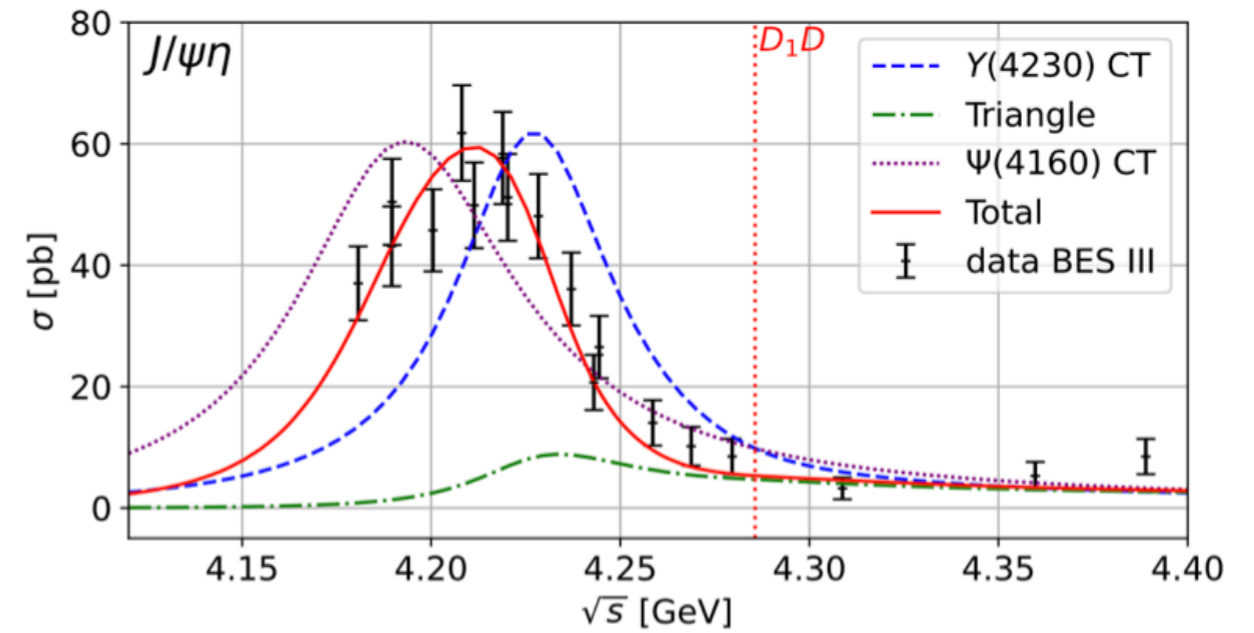


The $J/\psi\eta$, $\chi_{c0}\omega$, $X(3872)\gamma$ channels

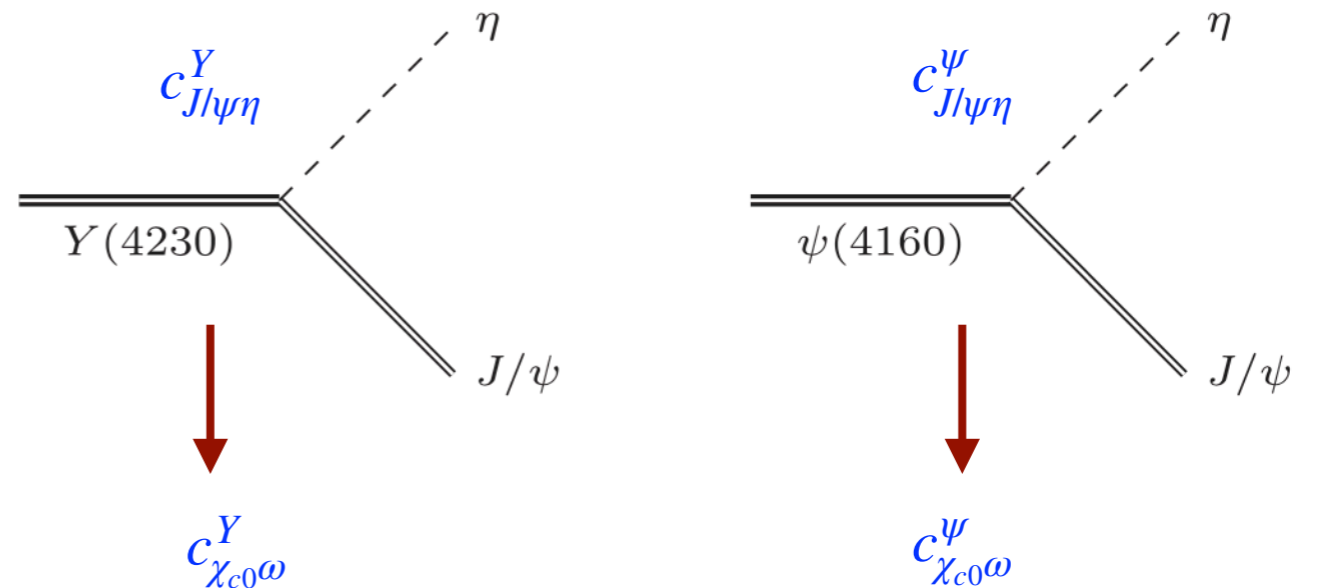
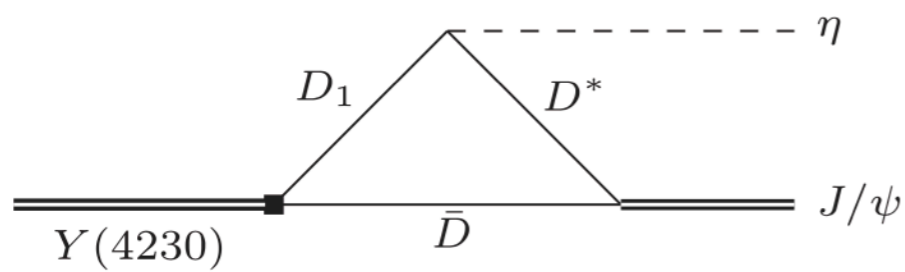
- The $J/\psi\eta$, $\chi_{c0}\omega$, $X(3872)\gamma$ line shapes



BESIII, PRL122(2019)232002

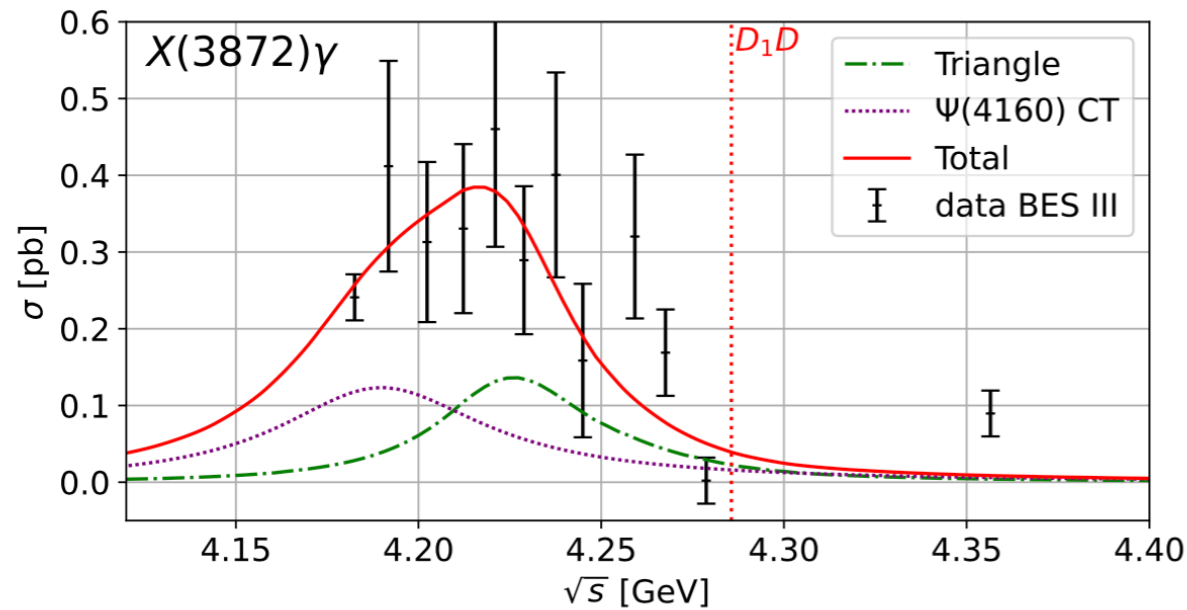


BESIII, PRD102(2020)031101

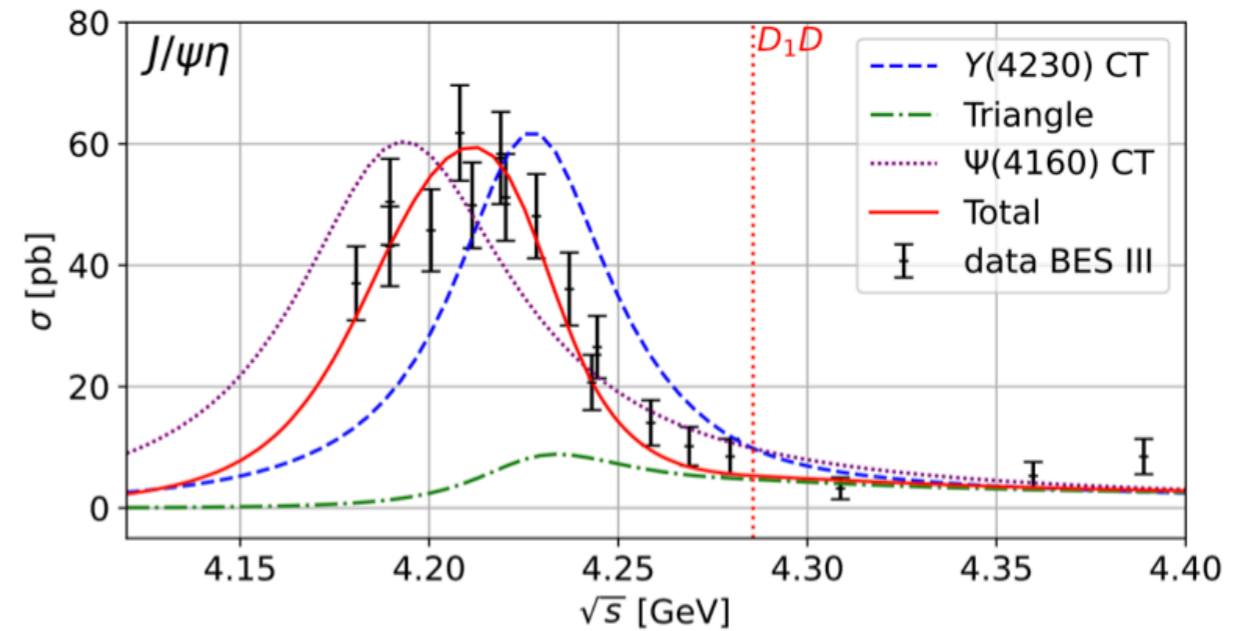


The $J/\psi\eta$, $\chi_{c0}\omega$, $X(3872)\gamma$ channels

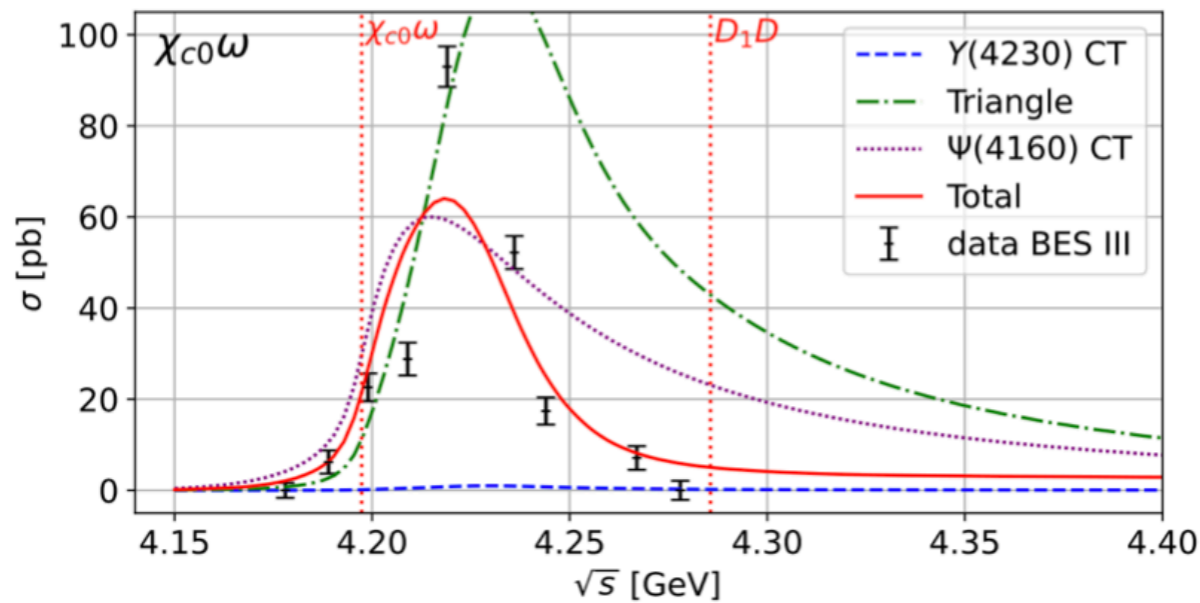
- The $J/\psi\eta$, $\chi_{c0}\omega$, $X(3872)\gamma$ line shapes



BESIII, PRL122(2019)232002



BESIII, PRD102(2020)031101

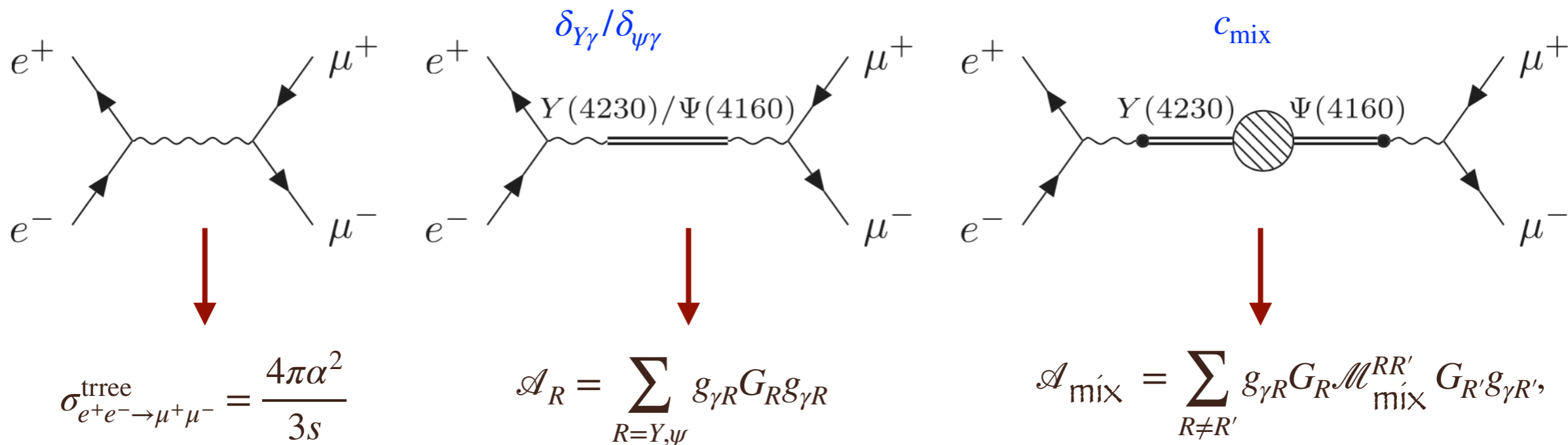


BESIII, PRD99(2019)091103

- ① Destructive in $\chi_{c0}\omega$
- ② Γ_ω is convoluted in $\chi_{c0}\omega$ channel
- ③ Constructive in $X(3872)\gamma$
- ④ Large statistic data is needed

The $\mu^+\mu^-$ channel

- $e^+e^- \rightarrow \mu^+\mu^-$ process



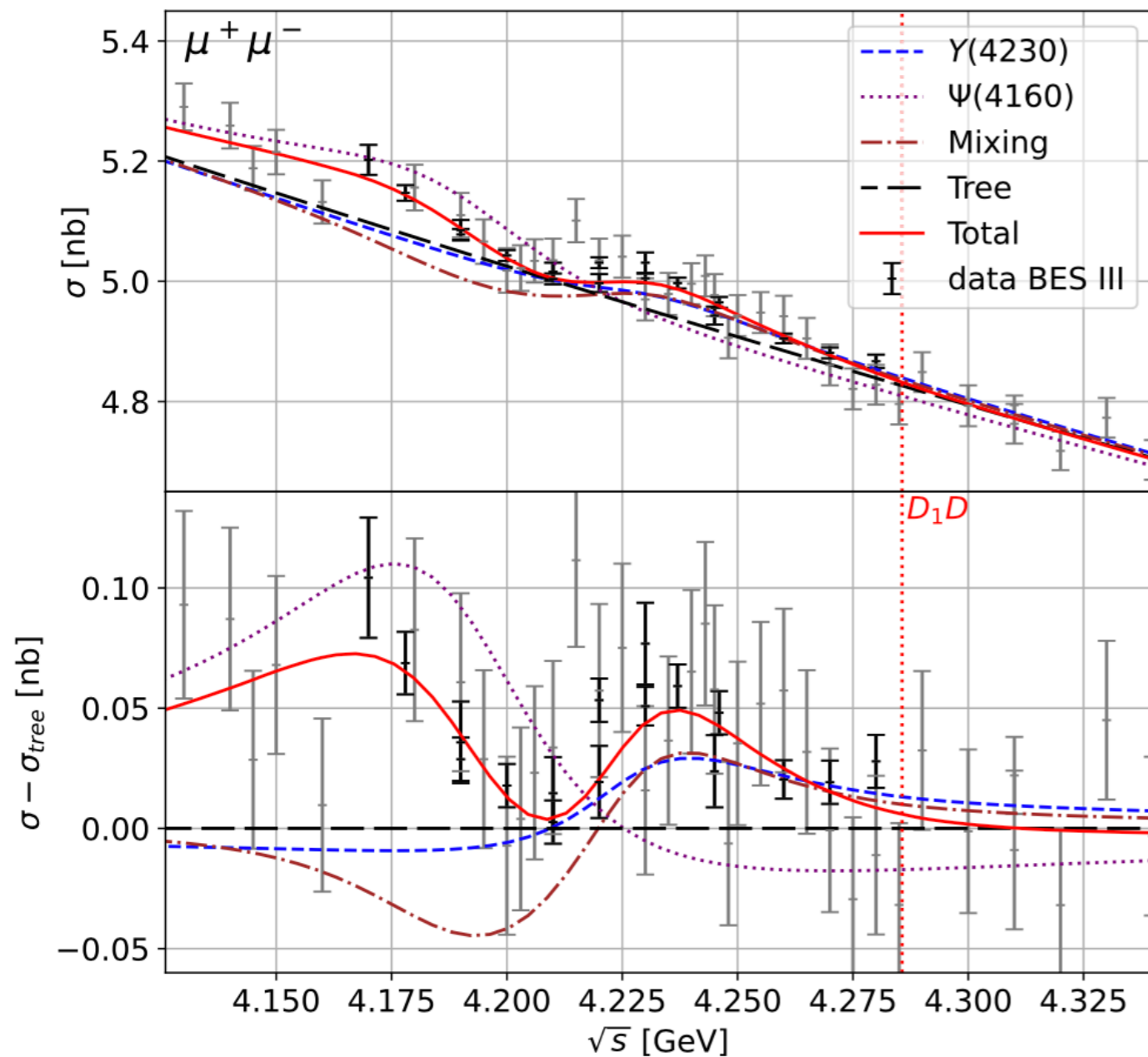
The cross section $\sigma_{e^+e^- \rightarrow \mu^+\mu^-} = \sigma_{e^+e^- \rightarrow \mu^+\mu^-}^{\text{tree}} \left| 1 + \mathcal{A}_R + \mathcal{A}_{\text{mix}} \right|^2$

With tree-level cross section subtracted

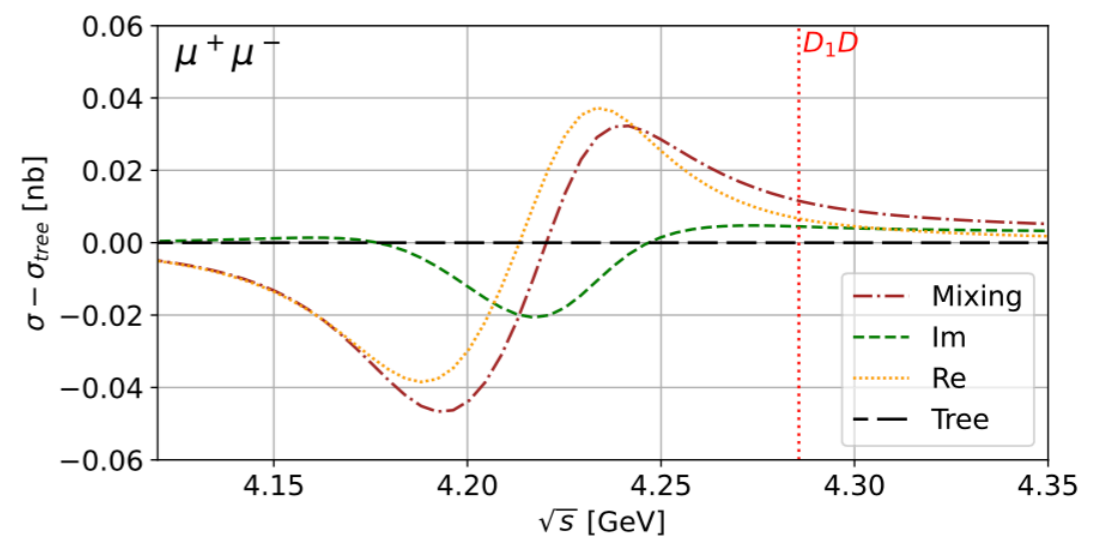
$$\sigma_{e^+e^- \rightarrow \mu^+\mu^-} - \sigma_{e^+e^- \rightarrow \mu^+\mu^-}^{\text{tree}} \approx 2\sigma_{e^+e^- \rightarrow \mu^+\mu^-}^{\text{tree}} \text{Re} \left(\mathcal{A}_R + \mathcal{A}_{\text{mix}} \right).$$

The $\mu^+\mu^-$ channel

- The $e^+e^- \rightarrow \mu^+\mu^-$ cross sections



BESIII, PRD102(2020)112009



- ① Re changes the sign between the two states
- ② The dramatic changes of the cross section indicate the existence of the $\psi(4160)$

Summary and outlook

- A global fit to eight channels in a phenomenological way
- A combined fit of all channels require the presence of the $\psi(4160)$
- A single vector charmonium-like state $Y(4230)$ exists in [4.2, 4.35] GeV region
- $M_{Y(4230)}^{\text{pole}} = (4227 \pm 4) - i(25_{-1}^{+4}) \text{ MeV}$, $M_{Z_c(3900)}^{\text{pole}} = 3884 - 22i \text{ MeV}$
- Asymmetric lineshape stems from the $D_1\bar{D}$ threshold



- A framework in EFT point of view
- Full $\pi\pi - K\bar{K}$ FSI

Thank you very much for your attention!